In Search of Late-Stage Planetary Building Blocks

Richard J. Walker, Katherine Bermingham, Jingao Liu*, Igor S. Puchtel, Mathieu Touboul** and Emily A. Worsham

Corresponding Author – Richard J. Walker (rjwalker@umd.edu)

Isotope Geochemistry Laboratory
Department of Geology
University of Maryland
College Park, MD 20742 USA

Present Address:

*1-26 Earth Sciences Building, Department of Earth and Atmospheric Sciences
University of Alberta, Edmonton, Alberta, Canada T6G 2E3

**Laboratoire de Géologie de Lyon, Ecole Normale Supérieure de Lyon, Labex LIO, Université Lyon 1, 46 Allée d'Italie 69364 Lyon Cedex 7, France

12,737 Words (Abstract + Text)

Revision Submitted to: *Chemical Geology*
December 21, 2021

Abstract

Genetic contributions to the final stages of planetary growth, including materials associated with the giant Moon-forming impact, late accretion, and late heavy bombardment are examined using siderophile elements. Isotopic similarities between the Earth and Moon for both lithophile and siderophile elements collectively lead to the suggestion that the genetics of the building blocks for Earth, and the impactor involved in the Moon-forming event were broadly similar, and shared some strong genetic affinities with enstatite chondrites. The bulk genetic fingerprint of materials subsequently added to Earth by late accretion, defined as the addition of ~0.5 wt. % of Earth's mass to the mantle, following cessation of core formation, was characterized by $^{187}Os/^{188}Os$ and Pd/Ir ratios that were also similar to those in some enstatite chondrites. However, the integrated fingerprint of late accreted matter differs from enstatite chondrites in terms of the relative abundances of certain other HSE, most notably Ru/Ir. The final ≤0.05 wt. % addition of material to the Earth and Moon, believed by some to be part of a late heavy bombardment, included a component with much more fractionated relative HSE abundances than evidenced in the average late accretionary component.

Heterogeneous $^{182}W/^{184}W$ isotopic compositions of some ancient terrestrial rocks suggest that some very early-formed mantle domains remained chemically distinct for long periods of time following primary planetary accretion. This evidence for sluggish mixing of the early mantle suggests that if late accretionary contributions to the mantle were genetically diverse, it may be possible to isotopically identify the disparate primordial components in the terrestrial rock record using the siderophile element tracers Ru and Mo.

Keywords: building blocks, giant impact, late accretion, late heavy bombardment, siderophile elements

1. Introduction

The origins of the rocky planets, especially with regard to assembly processes and the chemical nature of their building blocks, have been the topic of intense interest and debate for decades. It is now generally agreed that the terrestrial planets were built as a result of a three stage process, initially consisting of the growth of planetesimals from dust, followed by the collisions of bodies of increasingly greater mass to create planetary embryos, culminating in the collision and accretion of the embryos to form planets during a giant impact stage of growth (e.g., Kokuba and Ida, 1998; Raymond et al., 2006; Morbidelli et al., 2012; Raymond et al., 2013). The final stage of major growth for the Earth likely occurred with the giant impact of a body comprising 5 wt. % or more of the mass of the present Earth, leading to the formation of the Moon (Hartmann and Davis, 1975; Canup and Asphaug, 2001; Canup, 2012; Ćuk and Stewart, 2012; Reufer et al., 2012). Minor accretion amounting to ~0.5 wt. % of the present Earth's mass continued after this event (Kimura et al., 1974; Chou, 1978).

In addition to constraining the dynamical processes involved in the construction of the rocky planets, it is equally important to assess the origins and chemical nature of the materials from which the planets were built. Comparisons of the bulk compositions of the terrestrial planets have commonly been made on the basis of chemical models developed for these planetary bodies, most notably the Earth, Moon, and Mars; that is, bodies from which we are reasonably confident we have samples. Such models often require the assumption that the bodies were constructed from a combination of materials that were compositionally similar to the

47 primitive meteorites present in our collections (Wänke and Dreibus, 1988; 1994; McDonough
48 and Sun, 1995; Wänke, 2001; Taylor et al., 2006). The bulk planetary concentrations of a
49 number of poorly-constrained elements have been estimated by applying bootstrapping methods
50 which assume that the ratios of these elements to relatively well-constrained, geochemically-
51 comparable major elements, are similar to the ratios observed in primitive meteorites (e.g.,
52 McDonough and Sun, 1995). Models of the chemical composition of inaccessible planetary
53 reservoirs, such as Earth's core, often require these types of general assumptions (McDonough,
54 2003). Of course, it is unlikely that our meteorite collections sample the full compositional range
55 of primitive materials involved with planetary accretion. Thus, some limitations in bootstrapping
56 methods must be recognized. To circumvent this problem when assessing the compositions of
57 some elements in inaccessible planetary reservoirs, such as cores, abundances can also be
58 estimated by reverse modeling, using known or assumed mantle concentrations, and applying
59 appropriate metal-silicate distribution coefficients. Models of this type, however, must make
60 assumptions about the conditions of progressive metal-silicate segregation in a growing body
61 (e.g., Rubie et al., 2011).

62 The chemical and genetic makeup of the rocky planets can potentially be further
63 constrained by isotopic comparisons to one another and to primitive meteorites. For example,
64 planetary materials exhibit a large range in mass independent variations in $\Delta^{17}O$ (the *per mil*
65 deviation in $^{17}O/^{16}O$ from the terrestrial fractionation line), which can be used as genetic
66 fingerprints of precursor materials. It has been hypothesized that the heterogeneities in $\Delta^{17}O$
67 originated as a result of self-shielding effects in the photo-dissociation of CO by exposure to
68 ultraviolet light within the solar nebula (e.g., Thiemens and Heidenreich, 1983; Clayton, 2002;
69 Lyons and Young, 2005). Variations in $\Delta^{17}O$ among differentiated bodies have, therefore,

commonly been interpreted to reflect the formation of precursor materials at greater or lesser distances from the Sun, possibly coupled with time of formation (e.g., Yurimoto and Kuramoto, 2004). As an example of the application of O isotopes to issues of genetics, the similarity in the $\Delta^{17}O$ of the Earth and enstatite chondrites has commonly been interpreted to indicate that the major building blocks of the Earth formed in a region of the protoplanetary disk similar to where enstatite chondrites formed (Clayton et al., 1984; Javoy et al., 2010). Conversely, differences in the $\Delta^{17}O$ compositions of the Earth and Mars have been cited as evidence that the building blocks of these two bodies differed substantially (Franchi et al., 1999). Although there appears to be no perfect fit of all physical parameters between any types (or likely any combination of types) of primitive meteorites and the Earth, Moon or Mars, constraining the general categories of accretionary materials, nevertheless, remains an important objective of cosmochemistry.

Here, we focus mainly on the final ~10 to ~≤0.05 wt. % of Earth's accretion. Late stages of major terrestrial planetary accretion may have included the participation of materials that formed in different portions of the protoplanetary disk, and included water- and organic-rich materials (Weidenschilling et al., 1997; Chambers, 2001; 2004). Thus, although limited in mass, late stage planetary growth may have had a disproportionate effect on the volatile contents of the rocky planets (e.g., Kerridge, 1985; Balsiger et al.; 1995; Eberhardt et al., 1995; Albarede et al., 2013; O'Brien et al., 2014; Rubie et al., 2015a). Further, late stage additions may have carried genetically distinct elemental and isotopic fingerprints. Here we use the term *genetic* to mean chemical and especially isotopic compositions of the the primary nebular materials from which an object was built. Because of the comparatively limited mass contributed by these processes, elemental and isotopic tracers comprising major elements, such as O, are of limited value in constraining the nature of these final building blocks. Thus, we will instead explore the possibility of tracing the

93 late-stages of planetary growth using insights gained from elemental and isotopic variability of
94 so-called *siderophile*, or Fe-loving, elements.
95 In this overview, the elemental and isotopic fingerprints of late stage building blocks that
96 may be recorded in mantle rocks from the Earth, as well as mantle-derived and impact generated
97 rocks from Mars and the Moon, respectively, will be examined. In addition to considering the
98 average elemental and isotopic characteristics of siderophile elements contained in the silicate
99 portions of these bodies, we will also explore the possibility that the signals of individual
100 building blocks might be identified through small differences in the isotopic compositions of the
101 siderophile elements Ru and Mo, which varied among early solar system materials as a result of
102 their incorporating differing proportions of diverse nucleosynthetic components. The basis for
103 this optimism is the discovery that primordial mantle heterogeneities, recorded by lithophile,
104 atmophile and siderophile short-lived radiogenic isotope systems, survived long enough to be
105 preserved in the terrestrial rock record (Caro et al., 2003; Willbold et al., 2011; Mukhopadhyay
106 et al., 2012; Touboul et al., 2012; 2014). If the interpretations of long-lived chemical/isotopic
107 heterogeneity in the mantle presented by these studies are correct, isotopically distinct domains
108 within the mantle, imparted during late stage accretion of genetically distinct materials, might
109 also be preserved in the rock record.
110
111 **2. Overview of Siderophile Elements**
112 Siderophile elements are those elements that strongly partition into liquid metallic Fe
113 relative to silicate melt, and are consequently concentrated, to greater or lesser extents, in the
114 cores of the rocky planets (Goldschmidt, 1937). Because of this, their concentrations in silicate
115 mantles and crusts are low compared to primitive meteorites, the compositions of which are

116 presumed to be representative of the majority of the planetesimals involved in the final stages of
117 rocky planet accretion (Anders and Grevesse, 1989). Siderophile trace elements are commonly
118 divided into sub-groups based on the intensity of their siderophilic tendencies under the typical 1
119 atmosphere experimental conditions initially employed to characterize the nature of metal-
120 silicate partitioning of these elements (e.g., Kimura et al., 1974; Borisov et al., 1994). The
121 moderately siderophile elements (MSE), including W, Co, Ag, Ni, Ge, and Mo, are characterized
122 by metal-silicate D values (concentration ratio of an element in liquid metal to liquid silicate)
123 ranging from about 10 to 1000. The highly siderophile elements (HSE), including Re, Os, Ir, Ru,
124 Pt, Rh, Au and Pd, are characterized by D values greater than 10,000.
125 One important characteristic of siderophile elements is that the intensity of their
126 siderophilic behavior can shift considerably at increasingly higher temperatures and pressures
127 (e.g., Ringwood, 1966; Murthy, 1991; Li and Agee, 1996; Holzheid et al., 2000). The general
128 tendency of most, but not all, siderophile elements is towards lower D values, as pressure and
129 temperature conditions increase (Righter and Drake, 1997; Mann et al., 2012). Their partitioning
130 characteristics are also affected by other intensive parameters of a given planetary body, such as
131 oxygen fugacity (fO_2), as well as the compositions of the participating metal and silicate phases
132 (Cottrell and Walker, 2006; Wade and Wood, 2005; Wade et al., 2012). These shifts in
133 partitioning behavior are important to recognize when considering issues of planetary growth and
134 core formation. Depending upon the conditions at which metal last equilibrated with silicates,
135 during progressive core formation in a growing body, appropriate D values likely changed
136 considerably during the growth of sizable planetary bodies, thus, affecting the final absolute and
137 relative concentrations of the siderophile elements in these mantles (e.g., Wade and Wood, 2005;
138 Rubie et al., 2011).

For the purposes of genetic tracing of late stage building blocks, it is also important to recognize that the processes leading to the present abundances of the MSE contained within the silicate portions of the rocky planets may not have been the same as for the HSE. The chondrite-normalized abundances of the MSE estimated for the bulk silicate Earth (BSE) vary considerably (**Fig. 1**). Experimental studies have shown that the abundances of many of the MSE can be accounted for if metal-silicate equilibration occurred at elevated temperatures and pressures (e.g., Hillgren et al., 1994; Righter et al., 1997; Li and Agee, 2001; Mann et al., 2009; Siebert et al., 2011; Wade et al., 2012). Thus, numerous studies have concluded that the abundances of these elements are consistent with metal-silicate equilibration at an average depth equivalent to pressures of 20-60 GPa. A major shift in fO_2 of the terrestrial mantle, resulting from either the disproportionation of ferrous iron into ferric iron plus metal, as occurs in Bridgmanite at high pressure (Frost et al., 2004; Frost and McCammon, 2008), or the partitioning of Si into core-forming metal, has also been proposed as having had a significant influence on the final concentrations of the MSE in the Earth's mantle (e.g., Wade and Wood, 2005; Rubie et al., 2011; 2015b).

In contrast to the MSE, the HSE occur in approximately chondritic relative proportions in the bulk silicate Earth (BSE) (**Fig. 1**) (Chou, 1978; Morgan, 1986; Meisel et al, 2001; Becker et al., 2006; Fischer-Gödde et al., 2011), and absolute abundances are only ~200 times lower than bulk CI chondrite abundances (Morgan, 1986). Further, the $^{187}Os/^{188}Os$ and $^{186}Os/^{188}Os$ ratios estimated for the BSE, that reflect the long-term decay of ^{187}Re and ^{190}Pt (where $t_{½}$ for ^{187}Re and ^{190}Pt are ~42 and 450 Gyr, respectively), are also within the range of chondritic meteorites, thus providing a robust record for time-integrated chondritic Re/Os and Pt/Os (Morgan, 1985; Walker et al., 1997; Meisel et al., 2001; Brandon et al., 2006). These characteristics of the HSE in the

BSE do not appear to be the consequence of high pressure and temperature metal-silicate equilibration. Experimental studies have shown that large differences in the metal-silicate distribution coefficients of siderophile elements at relevant temperatures and pressures would have led to non-chondritic relative abundances in the mantle (Holzheid et al., 2000; Brenan and McDonough, 2009; Mann et al., 2012). This is observed for MSE but not for HSE (**Fig. 1**). Instead, the HSE may owe their presence in the BSE to continued accretion of planetesimals with bulk chondritic compositions, following core formation (Kimura et al., 1974; Chou, 1978). This process has been commonly termed the *late meteorite influx*, the *late veneer*, or *late accretion*. This terminology can be confusing because different authors have used the terms to mean different things. For example, some authors have used the terms "late veneer" and "late accretion" to describe all material accreted after the end of core formation, and all material accreted after the last giant impact, respectively (e.g., Jacobson et al. 2014; Morbidelli and Wood, 2015). If the giant impact was the last event that led to growth of the core, then the terms are synonymous. The term late accretion has even been used to include the final major stage of terrestrial growth by giant impact (e.g., Schönbächler et al., 2010). Henceforth, here we will use the term late accretion to mean all additions following cessation of core formation.

Late accretion is a viable mechanism to explain HSE abundances in the BSE because the addition of bodies with chondritic bulk compositions to silicate mantles would have led to the establishment of comparatively high absolute, and chondritic relative abundances of HSE in the affected mantles. In the case of Earth, mass balance constraints suggest that it would be necessary to add ~0.5 wt. % of the mass of the total Earth (~2 x 10^{22} kg) to the mantle by late accretion in order to account for present-day mantle HSE abundances (Walker, 2009). Implicit in such models are the assumptions that abundances of all HSE in the mantle were very low prior to

185 late accretion, and that any metal present in late stage impactors was ultimately oxidized and
186 incorporated in the mantle, so that the siderophile elements added to the mantle after core
187 formation remained in the mantle (Kimura et al., 1974). The late accretion hypothesis is
188 currently the only viable process to explain the HSE characteristics of the BSE (Walker, 2009).
189 Nevertheless, the hypothesis is not without weaknesses. For example, the considerable apparent
190 difference in HSE abundances in the BSE compared to the bulk silicate Moon is a potential
191 major problem that will be discussed in section 5.2.

192 Appealing to two distinct mechanisms for the establishment of siderophile elements in the
193 terrestrial mantle is not necessarily a conflict. Models such as those proposed by Wade and
194 Wood (2005) and Rubie et al. (2011; 2015a) would lead to the establishment of typically ≥90%
195 of the MSE abundances in the mantle by high pressure and temperature metal-silicate
196 partitioning. Repeated processing of metal through the mantle, as a result of growth by giant
197 impacts and the resulting multiple stages of magma ocean formation and evolution, would lead
198 to a biasing of the MSE present in the mantle today towards the mass added by the later major
199 stages of accretion (Azbel et al., 1993; Kramers, 1998; Rubie et al., 2011, 2015b). For example,
200 calculations using the progressive growth model of Kramers (1998) suggest that ≥80% of the W
201 present in the mantle today was added by accretion of the final 10-20 wt.% of the Earth. By
202 comparison, mass balance constraints suggest that late accretion of ~0.5 wt. % mass addition
203 would add >95% of the HSE, but a maximum of only about 10% of an MSE, such as W, to the
204 mantle total. Thus, as noted by Dauphas et al. (2004), the genetics of the MSE present in the
205 mantle are not required to have been the same as the genetics of the HSE.
206
207

3. Isotopic Tracers

Two types of isotopic tracers of building blocks are considered here; radiogenic and nucleosynthetic. Long-lived radiogenic tracers have long proved to be useful for constraining the vigor and nature of mixing in the silicate portions of planets. For example, long-lived systems including ^{87}Rb-^{87}Sr, ^{147}Sm-^{143}Nd, ^{176}Lu-^{176}Hf, and ^{238,235}U-^{232}Th-^{206,207,208}Pb have been extensively used to trace mantle mixing over Earth history, particularly with respect to recycled crustal components (Zindler and Hart, 1986; Hofmann, 2003). Of the long-lived systems consisting of HSE, however, only the ^{187}Re-^{187}Os isotopic system, and to a lesser extent the ^{190}Pt-^{186}Os system, have been shown to be useful for characterizing late stages of planetary accretion to Earth, the Moon, and Mars (e.g., Morgan, 1985; Walker et al., 2002a; Meisel et al., 1996; Day et al., 2007; Brandon et al., 2012).

Short-lived radiogenic isotopic systems have much greater utility for examining the timing of early planetary accretion and differentiation processes with high resolution (e.g., Caro et al., 2003; Foley et al., 2005; Boyet and Carlson, 2005; Debaille et al., 2013; McLeod et al., 2014). Although short-lived isotopic systems, most notably the lithophile-atmophile ^{129}I-^{129}Xe system ($t_{½}$ = 15.7 Myr), the lithophile ^{146}Sm-^{142}Nd system ($t_{½}$ = 103 Myr), and the lithophile-siderophile ^{182}Hf-^{182}W system ($t_{½}$ = 8.9 Myr), were initially pursued primarily to date cosmochemical materials and processes, radiogenic decay of these systems has also led to the production of long-term isotopic heterogeneity in an array of sizable cosmochemical reservoirs, including the lunar and martian mantles (Nyquist et al., 1995; Foley et al., 2005; Debaille et al., 2009). Consequently, variations in the abundances of the daughter isotopes can also serve as tracers of planetary mantle mixing. Because the parent isotopes of these systems were extant for relatively short periods of time, ranging only from about 60 Myr for ^{182}Hf, to as long as 600 Myr for ^{146}Sm,

231 the heterogeneities they record can only have formed early in solar system history. For example,
232 the large differences in $^{182}W/^{184}W$ and $^{142}Nd/^{144}Nd$ isotopic ratios between nakhlite and
233 shergottite meteorites, with both groups presumably derived from the martian mantle, can only
234 be explained as a result of a major, possibly global, differentiation event within the first 15 to100
235 million years of solar system history (Foley et al., 2005; Debaille et al., 2009). Little subsequent
236 mixing between the mantle domains, from which the precursor melts to these rocks originated,
237 has evidently occurred.

238 Of major significance to the possibility of identifying late-stage building blocks of Earth is
239 the detection of small isotopic anomalies in all three radiogenic isotope systems, present in
240 materials derived from the terrestrial mantle (e.g., Caro et al., 2003, 2006; Willbold et al., 2011;
241 Mukhopadhyay, 2012). Here, the term anomaly refers to an isotopic composition that differs
242 from that of the dominant composition measured for modern terrestrial samples. The existence of
243 these anomalies highlights the long-term survival of isotopically-distinct mantle domains, some
244 of which likely formed within the first 50 million years of solar system history. With regard to
245 identifying building blocks, the reasoning applied here is that if radiogenic isotope anomalies
246 that formed very early in Earth history survived hundreds of millions to billions of years, then
247 nucleosynthetic isotopic heterogeneities, introduced to the mantle through the incorporation of
248 genetically diverse building blocks during the period of late accretion, might also have survived
249 and ultimately been incorporated into the rock record.

250 The application of nucleosynthetic anomalies as tracers of building blocks is based on the
251 observation that the isotopic compositions of numerous elements present in presolar grains
252 reflect diverse formational pathways in high energy, stellar environments. Nucleosynthetic
253 processes include *slow* neutron capture, or the *s*-process, such as by He burning in the outer shell

of an asymptotic giant branch star; *rapid* neutron capture, or the *r*-process, such as during a Type II supernovae; and by *proton* enrichment, or the *p*-process, such as by photo-disintegration of heavy elements or neutrino interactions (Burbidge et al., 1957). Evidence for each of these nucleosynthetic processes has been confirmed through the observation of predicted, large-scale isotopic enrichments and depletions in diverse presolar grains extracted from low metamorphic-grade primitive meteorites (e.g., Zinner, 1998; Nittler, 2003). In addition to direct measurements of nucleosynthetic variations in presolar grains, information regarding the identity and origin of presolar materials has also been obtained through chemical leaching of bulk primitive meteorites, followed by separate analysis of leachates and residues (Dauphas et al., 2002a; Hidaka et al., 2003; Schönbächler et al., 2005; Yokoyama et al., 2010).

Although the isotopic variability observed among presolar components was greatly attenuated by nebular mixing processes, some elements continued to remain isotopically heterogeneous during the formation of moderate-sized bodies. For example, Yin et al. (2002) and Dauphas et al. (2002b) reported isotopic variations on the order of several parts per ten thousand for the MSE Mo, in bulk samples of chondrites and iron meteorites. Some of these iron meteorites have been interpreted to sample the cores of diverse asteroidal- to embryonic-size bodies, in certain cases with diameters that may have exceeded 300 km (Yang et al., 2008). More recently, Burkhardt et al. (2011) reported a comparable range of mass independent Mo isotopic compositional variability among iron meteorites, chondrites and pallasites (**Fig. 2a-b**). Similarly, Chen et al. (2010) reported comparably large ^{100}Ru isotopic heterogeneities among iron meteorite and chondrite groups (**Fig. 3a-b**). The causes for such large-scale isotopic heterogeneity remain debated, but can include the preferential concentration of some types of presolar components into parent bodies, resulting from thermal or physical sorting mechanisms

277 of host phases in the solar nebula (Trinquier et al., 2007; Regelous et al., 2008). Alternatively,
278 these large-scale nucleosynthetic anomalies could reflect injections of diverse nucleosynthetic
279 materials from nearby supernovae at different times during the evolution of the nebula (Bizzarro
280 et al., 2007), followed by incomplete homogenization of these materials in the nebula (Carlson et
281 al., 2007; Andreasen and Sharma, 2007). Regardless of the true cause, the evidence for isotopic
282 heterogeneity in nucleosynthetic componentry among diverse planetesimals is strong.
283
284 In summary, like mass independent isotopic differences in O isotopes, the primordial
285 isotopic variations present for some siderophile elements in planetesimals mean that these
286 elements can serve as genetic tracers of the building blocks of planetary objects. Unlike O
287 isotopes, or the isotopic compositions of other lithophile trace elements, however, the siderophile
288 element isotopic fingerprints should be particularly useful for assessing the genetic makeup of
289 materials added to planetary bodies during the final stages of assembly.
290
291 **4. The Final ~10 wt. % of Accretion**
292 The canonical model for the formation of the Moon involves a giant impact of an impactor
293 comprising approximately 10% of the mass of the Earth (Canup and Asphaug, 2001). Although
294 recent models for the putative giant impact have expanded the possible range for the mass of the
295 impactor from as little as 5% (Ćuk and Stewart, 2012) to as much as 45% of the current mass of
296 the Earth (Canup, 2012), there is little doubt that it was the final major accretionary addition to
297 Earth. The event led to the transit of most of the metal from the impactor core through the
298 Earth's mantle. As a consequence, it could also have led to a substantial modification of
299 siderophile element abundances and their isotopic compositions retained in the silicate portion of

300 the Earth, following the impact (e.g., Halliday, 2004; Rubie et al., 2011). As evidenced by the
301 mass balance constraints discussed above, subsequent late accretion could not have modified the
302 abundances of the MSE in the mantle by more than ~10%. Thus, the giant impact would have
303 been the last major event involved in the establishment of the modern characteristics of MSE in
304 the terrestrial mantle. Consequently, some characteristics of MSE in the mantle today may
305 provide insights to the nature of the final giant impactor involved in the construction of the Earth
306 and Moon.

307 Of all the MSE, the modification of the mantle by giant impact has been most frequently
308 studied using W isotopes, because of the radiogenic tracer capability inherent in the system
309 (Halliday, 2004; Nimmo et al., 2010; Dwyer et al., 2014). Unfortunately, the W isotopic
310 composition of the mantle today can presently provide only limited constraints regarding the
311 nature of the giant impactor. This is because the outcomes of giant impact models involving the
312 Hf-W isotopic system are strongly dependent on assumptions about the timing of the impact, and
313 of core formation on both the proto-Earth and impactor. Of particular importance is the degree of
314 equilibration that occurred between the core of the impactor and the silicate Earth, as metal from
315 the impactor transited the mantle on its way to merge with the Earth's core (e.g., Halliday, 2004;
316 2008). In contrast to the W present in metal derived from the core of the impactor, it is assumed
317 that nearly all of the W present in the silicate portion of the impactor ended up mixing into the
318 terrestrial mantle, as well as being added to the silicate portion of the Moon.

319 With regard to metal-silicate equilibration, one endmember possibility is that the core of
320 the impactor quickly merged with the core of the Earth, with negligible exchange of W between
321 the merging core and the silicate Earth (**Fig. 4a**). In this case, the giant impact would likely have
322 led to an increase in the $\mu^{182}W$ (where $\mu^{182}W$ is the deviation in $^{182}W/^{184}W$ of a sample,

323 compared to a modern terrestrial standard, in parts per million) of the Earth's mantle as a result
324 of the addition of W from only the silicate portion of the impactor (Halliday, 2004). This is based
325 on the assumption that the $\mu^{182}W$ of the silicate portion of the impactor was more radiogenic than
326 the proto-Earth's mantle, because the embryo-size impactor is usually presumed to have accreted
327 and differentiated a core and mantle more rapidly than Earth, creating a high Hf/W mantle, while
328 ^{182}Hf was still plentiful (Dauphas and Pourmand, 2011). Thus, for this scenario, the $\mu^{182}W$ value
329 of the silicate Earth could have risen 100 ppm or more as a result of the impact (**Fig. 4a**).
330 The other endmember possibility is that a substantial portion of the core of the impactor
331 broke into small droplets, resulting from Rayleigh-Taylor instabilities, and the droplets
332 equilibrated with the surrounding silicate liquid as they sank through the mantle to merge with
333 the terrestrial core (Dahl and Stevenson, 2010). In this case, the W isotopic composition of the
334 silicate Earth would likely have decreased significantly (**Fig. 4b**), as W with low $\mu^{182}W$ from the
335 impactor core ($\leq$ -200) equilibrated with the presumably more radiogenic silicate Earth
336 (Halliday, 2008). In this case, the mantle of the Earth, just prior to the impact, may have been
337 $\geq$200 ppm more radiogenic than the present mantle.
338 Because of these uncertainties in the extent of equilibration between metal and silicate, it is
339 currently impossible to estimate the $\mu^{182}W$ value of the impactor mantle, as well as precisely
340 determine the average age of core formation (where 50 wt. % of the core mass is achieved) for
341 either the impactor or the proto-Earth. Nevertheless, W isotopes may have some utility in
342 deconvolving the processes that occurred during and after the giant impact. Most importantly, it
343 has been recently determined that the Moon has a $\mu^{182}W$ value that is enriched relative to the
344 Earth's mantle by 21-26 ppm (Kruijer et al., 2015; Touboul et al., 2015). The difference is most
345 parsimoniously explained by assuming the W isotopic composition of the Earth and Moon were

346 identical immediately following the coalescence of the Moon, and that the small difference is the
347 result of disproportional late accretion to the Earth and Moon, *after* the Moon formed. One major
348 ramification of this observation is that, in order for the W isotopes and HSE abundances of the
349 Earth and Moon to be self-consistent, the metal from the giant impactor had to have sufficiently
350 equilibrated with the Earth's mantle such that any pre-existing HSE in the proto Earth's mantle
351 were efficiently stripped from the mantle by this metal.

352 Given that the W isotopic composition of the Moon at the time of its formation was likely
353 inherited mainly from the giant impactor, it is problematic that it was identical to the proto
354 Earth's mantle. This is because it is unlikely that two, very different size bodies simultaneously
355 segregated cores in ways that resulted in mantles with nearly identical Hf/W, which is required to
356 generate identical W isotopic compositions. One possible explanation for the W isotopic
357 similarity between the Earth and Moon at the time of formation is that through happenstance, the
358 impactor and Earth formed from genetically similar materials, and had roughly similar average
359 core segregation ages (e.g., Dauphas et al., 2014). Another option is that the Earth's mantle and
360 the proto-lunar disk somehow chemically and isotopically equilibrated prior to lunar coalescence
361 (Pahlevan and Stevenson, 2007), as has been suggested by the similarity of isotopic
362 compositions for other elements, such as O, Ca, Ti, and Si (e.g., Wiechert et al., 2001; Trinquier
363 et al., 2009; Simon et al., 2010; Zhang et al., 2012; Fitoussi and Bourdon, 2012). Information
364 that is currently being gleaned about the drawdown of mantle HSE abundances at the time of the
365 giant impact (e.g., Kruijer et al., 2015; Touboul et al., 2015), coupled with an improved
366 understanding of the rate of isotopic versus elemental equilibration between metal and silicate,
367 may one day enable stronger constraints to be placed on the formation and differentiation history
368 of the impactor.

Another key genetic indicator of the final ~10 wt. % accretion of the Earth is Mo isotopic composition. As noted above, >50% of the Mo present in the mantle today was likely contributed during the final 10-20 wt. % accretion of Earth. Thus, the Mo isotopic composition of the mantle is an important fingerprint for late stages of major terrestrial accretion. Work to date suggests that the Mo isotopic composition of the silicate Earth differs from all known chondrite groups and most iron meteorite groups (Dauphas et al., 2002b; Burkhardt et al., 2011)(**Fig. 2a-b**). The only major meteorite group measured to high precision that perfectly matches the Mo isotopic composition of the silicate Earth, within the current level of precision, is the group IAB iron meteorites (Burkhardt et al., 2011). It has been proposed that this group of iron meteorites formed as a result of metal pooling at the base of an impact crater following an impact onto a primitive body (Wasson and Kallemyn, 2002). This iron group, however, shares little other elemental or isotopic commonality with the Earth. For example, the $\Delta^{17}O$ composition range of silicates present in IAB irons differs substantially from the Earth (Wasson and Kallemeyn, 2002). Therefore, even if their Mo isotopic compositions overlap, the group is probably not closely genetically related to Earth.

Enstatite chondrites have been touted by some as potential building blocks of the bulk Earth (e.g., Javoy et al, 2010). Compositionally, however, it has been noted that the enstatite chondrites have substantially different major element compositions (e.g., Mg/Si) compared to estimates for the composition of Earth's primitive mantle. So, unless there is a major hidden mantle reservoir with a substantially different bulk composition from the observed mantle, the enstatite chondrites cannot account for Earth's bulk composition (e.g., Palme and O'Neill, 2003). That said, enstatite chondrites are good to excellent genetic matches to the isotopic composition of the bulk Earth with respect to, e.g., O, Ti, Ca, and Ni (Clayton, 2004; Carlson et al., 2007;

392 Trinquier et al., 2009; Regelous et al., 2008; Herwartz et al., 2014). This means that building
393 blocks that were genetically similar to, but compositionally distinct from enstatite chondrites, are
394 implicated in the construction of the bulk Earth. Not all isotopic compositions that reflect genetic
395 componentry match, however. Fitoussi and Bourdon (2012) reported a ~30 ppm difference in the
396 Si isotopic composition between the silicate Earth and enstatite chondrites.

397 The Mo isotopic composition of enstatite chondrites overlap with the BSE within the
398 present level of analytical precision (Burkhardt et al., 2011) (**Fig. 2b**). Burkhardt et al. (2011),
399 however, noted that the characteristic w-shaped Mo isotope pattern for enstatite chondrites, as
400 with ordinary and carbonaceous chondrites, is consistent with minor *s*-process depletion
401 compared with the Earth. Thus, they concluded that the Mo isotopic compositions of enstatite
402 chondrites are similar to, but distinct from, terrestrial Mo. Unlike the genetic similarities for
403 elements like O, Ti, Ca and Ni, between the Earth and enstatite chondrites, which likely reflect
404 the genetic history of the major building blocks of Earth, the Mo isotopic composition is most
405 likely a reflection of the final 10-20 wt. % of accretion. Thus, the fact that all of these elements
406 have isotopic compositions similar or identical to enstatite chondrites suggests that >99% of the
407 accretion of Earth occurred without a major change in the genetic signature of the materials
408 contributing to growth.

409 Application of the MSE to study the nature of late stage building blocks is not limited to
410 Earth. The Mo isotopic compositions of two shergottites analyzed by Burkhardt et al. (2011)
411 overlap with the composition of the silicate Earth, so no genetic difference between these two
412 bodies can be detected at the current level of analytical resolution for this element. However, the
413 uncertainties on the measured Mo isotopic composition for these samples are relatively large.
414 Future refinement of the Mo isotopic composition of Mars, and determination of whether or not

415 it has a uniform isotopic composition, will be critical to assessing whether late stage additions to
416 the Earth and Mars came from genetically similar materials, and whether late stage building
417 blocks to Mars were well homogenized before the large-scale differentiation events that led to
418 isotopic heterogeneity in ^{182}W and ^{142}Nd.
419
420 In summary, the isotopic compositions of W in terrestrial and lunar rocks currently provide
421 little direct information about the giant impactor that was the final major building block of the
422 Earth. The data do, however, provide important new constraints on the physical processes that
423 occurred during this final major accretionary event. Most importantly, it appears that metal from
424 the impactor efficiently stripped HSE from the proto-Earth's mantle, such that the late
425 accretionary clocks for the reconstituted Earth, and newly coalesced Moon, began at the same
426 time. The Mo isotopic composition of the terrestrial mantle is likely dominated by Mo provided
427 by the building blocks that contributed the final 10-20 wt. % to Earth's mass. The Mo isotopic
428 composition of the mantle is very similar to enstatite chondrites, much like isotopic compositions
429 of other genetic tracers that reflect the composition of the bulk Earth. This suggests that the
430 building blocks of Earth were genetically similar to enstatite chondrites, and did not vary much
431 from a genetic standpoint over the course of the first >99% of Earth's construction.
432
433 **5. The Final ~0.5 wt. % of Accretion**
434 *5.1. Highly Siderophile Elements in the Bulk Silicate Earth*
435 The absolute and relative abundances of HSE in primitive meteorites vary among the major
436 chondrite groups (Walker et al., 2002a; Horan et al., 2003; Brandon et al., 2005; Tagle and
437 Berlin, 2008; Fischer-Gödde et al., 2010)(**Fig. 5**). For example, Pd/Ir in some enstatite chondrites

438 tend to be higher than for ordinary, carbonaceous, or R-type chondrites. Given that Re/Os also
439 varies among the chondritic groups, the $^{187}Os/^{188}Os$ of chondrites can serve as an important,
440 complementary parameter to discriminate among chondrite groups. Most notably, carbonaceous
441 chondrites are characterized by generally lower $^{187}Os/^{188}Os$, and therefore lower long-term
442 Re/Os, than ordinary and enstatite chondrites (**Fig. 6**). Modest, long-term differences in Pt/Os
443 have also resulted in small differences in $^{186}Os/^{188}Os$ among some chondrite groups (Brandon et
444 al., 2006), although the current level of resolution is insufficient for this system to be very useful
445 as a tracer.

446 Although variations in the relative abundances of HSE are becoming increasingly better
447 constrained for chondritic components (e.g., Horan et al., 2009; Archer et al., 2014), except for
448 calcium-aluminum rich inclusions, there has been only limited success in determining the causes
449 of the variations among the HSE characteristics of bulk chondrites (Mason and Taylor, 1982;
450 Sylvester et al., 1990; Fischer-Gödde et al., 2010). Thus, no nebular or parent body processes can
451 currently be firmly linked to the HSE characteristics observed in bulk chondrites. This means the
452 process that led to lower, long-term Re/Os in carbonaceous chondrites, compared to other
453 chondrite groups, may not be related to the accompanying, generally more volatile-rich nature of
454 carbonaceous chondrites. Despite these current limitations to fingerprinting late accretionary
455 additions, if most of the mass of HSE present in the BSE today was added as a result of late
456 accretion, the relative abundances of these elements in the BSE should provide an averaged
457 compositional snapshot of the final ~0.5% of mass addition to Earth.

458 Establishing HSE abundances in the BSE with sufficient precision to make comparisons to
459 possible cosmochemical precursors is problematic. Because of the sensitivity of $^{187}Os/^{188}Os$
460 ratios to discriminate among small, long-term differences in Re/Os, Os isotopes have been

especially heavily used among the HSE to characterize the Re/Os of the mantle (Hirt et al., 1963), and ultimately, the nature of late accreted materials to Earth (Morgan, 1985; Meisel et al., 1996; 2001). However, the application is not straightforward. Although Os is highly compatible within the mantle, the Os isotopic composition of the BSE cannot be measured directly via analysis of the dominant silicate reservoir in Earth, the oceanic mantle. This is because Re behaves incompatibly during mantle melting (Barnes et al., 1985; Rehkämper et al, 1999; Pearson et al., 2004). Consequently, oceanic and continental crustal extraction has modified the Re/Os of the residual oceanic mantle over Earth history. Abundances of Re estimated for the continental crust are relatively low (Peucker-Ehrenbrink and Jahn, 2001), and given the limited mass of this reservoir, its formation is unlikely to have led to significant modification of the Re/Os of the residual mantle. By contrast, the formation of oceanic crust, with its comparatively high Re concentrations, may have significantly modified the Re/Os of the residual mantle. The magnitude of this modification is open for debate, as some of the Re extracted into oceanic crust has been recycled back into the mantle. How much of the Re (and Pt) has been re-mixed back into the oceanic mantle remains difficult to assess (Walker et al., 2002b).

To circumvent this problem, Meisel et al. (1996; 2001) applied a projection method utilizing the compositions of variably melt-depleted mantle peridotite xenoliths to estimate the $^{187}Os/^{188}Os$ of the BSE. They plotted $^{187}Os/^{188}Os$ (record of long-term Re/Os) versus Al_2O_3 or Lu, indicators of mantle melt depletion that are not as easily modified by secondary processes as Re, and projected the resulting linear trends to points of intersection with assumed Al_2O_3 or Lu concentrations in the BSE. Using this method, Meisel et al. (2001) reported a $^{187}Os/^{188}Os$ ratio of 0.1296 ± 0.0008 (2σ). This ratio must be considered a *minimum* estimate because the projections were made mainly from samples derived from sub-continental lithospheric mantle. Such

peridotites must have been physically separated from the oceanic mantle at some time prior to isolation as sub-continental lithospheric mantle. The oceanic mantle itself was most likely variably depleted in Re prior to these reservoirs transitioning from oceanic to sub-continental lithospheric mantle, so the melt depletion events recorded in these rocks likely included at least one stage of prior melt depletion. The $^{187}Os/^{188}Os$ estimated for the BSE is at the upper end of the range of compositions recorded in bulk ordinary and enstatite chondrites (**Fig. 6**). Given this, the $^{187}Os/^{188}Os$ of the BSE appears to be most similar to ordinary and enstatite chondrites, or even slightly more radiogenic, and this likely means that carbonaceous chondrites, or similar materials, were not major players in late accretion (Walker et al., 2002a). This conclusion has subsequently been supported by arguments based on isotopic evidence for other elements (e.g., Jacobson et al., 2014). Given the volatile-rich nature of some carbonaceous chondrite groups, this observation in turn has been taken as evidence that late accretion provided little water to Earth (Drake and Righter, 2002), although as noted, there is currently no known process that relates the incorporation of volatiles and low Re/Os into the parent bodies of carbonaceous chondrites.

Absolute and relative abundances of other HSE have been estimated for the BSE using a similar approach as for $^{187}Os/^{188}Os$ (Becker et al., 2006; Fischer-Gödde et al., 2011). When collectively considering the HSE characteristics estimated for the BSE as compared with chondrites (**Fig. 7**), it appears to be most similar to enstatite chondrites for Re/Os, Os/Ir, Pt/Ir and Pd/Ir (Becker et al., 2006). However, the BSE appears to be modestly suprachondritic with respect to Ru/Ir and possibly Pd/Ir (Becker et al., 2006). It is possible that the slight Pd enrichment could be the remnant effect of high pressure-temperature metal-silicate partitioning as discussed with regard to the MSE (e.g., Mann et al., 2012). Current experimental data,

however, provide no evidence that this could also be true for Ru. Thus, although the current estimate of the HSE composition of the BSE is most like enstatite chondrites, it is not a perfect match to any known chondrite group, or individual chondrites present in our collections. This could mean that late accretion to Earth was dominated by one or more components that were somehow processed in the nebula, or on a parent body, such that HSE were fractionated relative to presently sampled chondrites. This in turn could occur as a result of the location of formation within a chemically heterogeneous protoplanetary disk, or formation at a different time in a chemically evolving nebula. Given that there are bulk chondrites with individual HSE ratios that extend beyond those estimated for the BSE (although no one chondrite has all of the HSE characteristics of the BSE), nebular or parent body processes can evidently cause such fractionations. It is also possible that the fractionated HSE abundances present in the dominant late accretionary component could result from another process, such as crystal-liquid fractionation of a metal component (e.g., Fischer-Gödde et al., 2011).

It is important to recognize that there are some limitations to the projection approach towards characterizing the BSE and fingerprinting late accretionary additions, using HSE. Of greatest concern is the precision and accuracy of HSE estimates for the BSE. The absolute and relative concentration estimates in the BSE are based on measurements of mantle peridotites that may represent the end stage of multiple processes, including mantle melting, metasomatism and crustal recycling (Alard et al., 2000; Le Roux et al., 2007). Thus, although the broadly chondritic nature of the BSE is of little doubt, the relatively small differences in elemental ratios that are key to discriminating among chondritic groups, or fingerprinting a heretofore unidentified chondrite-like contributor to the mantle, have been called into question (e.g., Lorand et al., 2009). The primary question is whether any mantle peridotites can provide sufficient fidelity in

recording the BSE composition. The typically strongly compatible natures of Os, Ir, and Ru, make them less susceptible to modification by partial melting and metasomatic processes, compared to Pt, and especially the incompatible Pd, Au, and Re. Consequently, they provide the strongest constraints on the HSE composition of the BSE, and the suprachondritic nature of Ru/Ir in the BSE appears to be real. Further, the similarity of HSE characteristics of large numbers of variably "fertile" mantle peridotites, ranging from abyssal peridotites, to peridotites from the mantle sections of ophiolites, to oceanic mantle xenoliths, supports the contention that the BSE is characterized by suprachondritic Ru/Ir and possibly Pd/Ir (Becker et al., 2006; Fischer-Gödde et al., 2011). However, compilation of an even larger number of data from all types of mantle lithologies, combined with an improved understanding of how HSE from oceanic crust have been recycled back into the oceanic mantle, may ultimately be required to assemble a high-confidence understanding of HSE in the BSE.

The most promising element for examining the genetic characteristics of late accreted HSE is Ru. As a HSE, Ru was strongly concentrated into metal by core formation processes. As noted above, the large range of nucleosynthetic isotopic compositions recorded in meteorites (Chen et al., 2010) makes this element ideal as a genetic tracer of cosmic materials contributed by late accretion. To date, Ru data for terrestrial rocks and meteorites are very limited. However, the most recent results (Fischer-Gödde et al., 2014; Bermingham et al., 2015) suggest that, as with Mo, the isotopic composition of Ru in the BSE is very similar to enstatite chondrites, and is well resolved from all carbonaceous chondrites. This observation is then consistent with the Os isotopic results.

5.2. Constraining the Physical Nature of Late Accretion

553 One key aspect of utilizing siderophile elements as genetic tracers of planetary building
554 blocks requires knowledge of the specific physical processes involved in their incorporation into
555 planetary mantles. This is especially true for the HSE. For example, late accretion of HSE to
556 Earth's mantle may have occurred as a consequence of a relatively gentle rain of smaller bodies
557 onto the surface of the planet, as envisioned by some workers (Anders, 1968; Turekian and
558 Clark, 1969). This concept led to the coining of the term *late veneer*, as discussed above. In this
559 case, a dog's breakfast of HSE-rich materials of diverse genetics may have been slowly mixed
560 downward into the mantle as a result of crustal recycling, coupled with mantle convection. One
561 way to test this hypothesis would be to look at the evolution of HSE abundances in the Archean
562 mantle using high-degree partial melts that extract large proportions of HSE from the mantle and
563 experience little to no fractionation *en route* to the surface, such as komatiites. Komatiites are
564 high MgO lavas, which are commonly presumed to be derived from partial melting in deep
565 mantle upwellings, or plumes (Campbell et al., 1989). Maier et al. (2009) argued that gradual
566 downward mixing of late accreted materials can potentially account for the low abundances of
567 HSE in some early Archean komatiites, and that the "normal" HSE abundances found in
568 komatiites formed later than ~2.9 Ga indicate that the putative late accreted materials had
569 become well-mixed into the deep mantle sources of komatiites by that time.
570 The combined HSE abundances and Re-Os and Pt-Os isotopic studies have resulted in
571 robust estimates of HSE abundaces in deep mantle sources of komatiites, ranging in age from 3.6
572 to 2.4 Ga using the projection technique (Puchtel et al., 2004), whereas the ^{187}Re-^{187}Os and ^{190}Pt-
573 ^{186}Os isotopic systematics confirmed post-crystallization, closed-system behavior of the rocks
574 with respect to HSE abundances (Puchtel et al, 2009). The Os isotopic evidence for closed
575 system behavior provides some additional confidence that the projected mantles source

576 abundances are accurate. The relative HSE abundances obtained for the late Archean komatiite
577 systems were concluded to be best matched by those in enstatite chondrites (e.g., Puchtel et al.,
578 2004a,b; 2009a).The komatiite systems studied in this manner show significant variations in the
579 absolute HSE abundances between the sources of late Archean komatiite systems (**Fig. 8**), but
580 are generally similar to those in the sources of early Archean komatiite systems, indicating little
581 temporal changes in the HSE abundances (Puchtel et al., 2014). There are notable exceptions,
582 however, with the oldest early Archean komatiite system (3.55 Ga Schapenburg) having
583 substantially lower HSE abundances compared to all other komatiite systems studied to-date,
584 which was interpreted to reflect sluggish mixing of post-magma ocean domains in the Archean
585 mantle (Puchtel et al., 2009b).

586 Another way to advance understanding of the physical nature of late accretion is by
587 combining observations of the chemical characteristics of planetary materials with dynamical
588 models for the first ~500 million years of solar system history. Here, comparing the
589 characteristics of the HSE present in the terrestrial mantle with abundances present in the lunar
590 and martian mantles may be particularly important. The abundances and isotopic compositions
591 of the HSE in at least the upper portion of the terrestrial mantle are generally well defined and
592 limited in variation. As noted, the $^{187}Os/^{188}Os$ and $^{186}Os/^{188}Os$ ratios estimated for the BSE are
593 within the range of chondritic meteorites (Meisel et al., 2001; Walker et al., 1997; Brandon et al.,
594 2006). Further, data for the global sampling of oceanic and subcontinental lithospheric mantle
595 peridotites are characterized by relatively uniform abundances of Os and Ir, two HSE that are
596 highly compatible during partial melting of the mantle (e.g., Rehkämper et al, 1999; Morgan et
597 al., 2001). While there has long been a question as to whether the upper mantle is more enriched
598 in HSE than the lower mantle, seismic tomography over the past 20 years has documented the

599 exchange of matter between upper and lower mantle, providing evidence for mantle plumes
600 rising from the lower mantle and subducting slabs transiting into the lower mantle (e.g., Goes et
601 al., 1999; Nolet et al., 2006). It is, therefore, likely that there are presently no major, global-scale
602 HSE concentration variations within the mantle. Consequently, uncertainty in the mass of late
603 accreted materials to the mantle, necessary to account for the observed abundances of HSE,
604 primarily reflects the factor of two variation in HSE abundances between different types of
605 chondritic meteorites (e.g., Horan et al., 2003), rather than uncertainties in the HSE content of
606 the mantle.

607 It is much more difficult to constrain the abundances of the HSE in the lunar and martian
608 mantles compared to the terrestrial mantle. No mantle samples have, as yet, been collected from
609 either body. Hence, mantle abundances of the HSE must be deduced from mantle-derived
610 volcanic rocks. Based on HSE abundances present in leached samples of picritic glass spherules
611 and lunar basalts, Walker et al. (2004) and Day et al. (2007), respectively, estimated that HSE
612 concentrations in the lunar mantle are a factor of 20 or more lower than in the terrestrial mantle
613 (**Fig. 9a**). Such a large difference in concentration, if correct, cannot be explained by
614 gravitational focusing or inefficiency of impactor retention. The lower concentrations may
615 instead reflect proportionally much less mass added to the lunar mantle by late accretion,
616 compared to the Earth. This in turn could result from a longer period of late accretion for Earth,
617 compared to the Moon, i.e., one that began well before formation of the Moon. However, as
618 noted above, recent W isotopic data for the Moon suggest that the Moon-forming giant impact
619 efficiently removed HSE from the mantle to Earth's core and reset the late accretionary clock for
620 the two bodies (Kruijer et al., 2015; Touboul et al., 2015). If so, this means that the dominant late
621 accretionary periods of the Earth and Moon began after formation of the Moon, and were

622 contemporaneous. Unless substantial quantities of late accreted materials to the Moon are
623 sequestered from our view in its lower crust (e.g., Schlichting et al., 2012), an interpretation for
624 which there is currently no physical evidence, there remains a sizable mismatch in the
625 proportions of late accreted materials added to the mantles of the Earth and Moon. As noted by
626 Walker (2009) this mismatch presents a potential problem for the late accretion hypothesis.
627 In contrast to the lunar mantle, the martian mantle appears to have HSE abundances that
628 are surprisingly similar to those present in the terrestrial mantle. Basaltic and ultramafic
629 shergottite meteorites, commonly believed to come from Mars, are characterized by HSE
630 abundances that scale with the MgO content of the rocks in a way that is similar to terrestrial
631 volcanic rocks (Brandon et al., 2012)(**Fig. 9b**). In addition, shergottites exhibit a range of initial
632 $^{187}Os/^{188}Os$ that is very similar to the range of compositions present in terrestrial mantle-derived
633 volcanic rocks (Brandon et al., 2012). Given the fact that Mars is commonly presumed to have
634 formed as a planetary embryo prior to the Earth (Dauphas and Pourmand, 2011), it might be
635 expected to have a larger proportion of late accreted material mixed throughout its mantle.
636 Instead, all existing data suggest that the HSE concentrations in the martian mantle are similar to
637 those in the terrestrial mantle, indicating that a roughly similar proportion of late accreted
638 materials was added to the mantle of Mars (Brandon et al., 2012).
639 Bottke et al. (2010) reported that one way to account for the similarity of HSE abundances
640 in the terrestrial and martian mantles, but much lower HSE abundances in the lunar mantle is by
641 a process they termed *stochastic late accretion*. The principle of stochastic late accretion is based
642 on the assumption that most late accretionary mass was added to the Earth and Mars by a very
643 limited number of impacts of approximately Pluto mass bodies (~1 x 10^{22} kg). By chance, the
644 Moon was not struck by any bodies of this size, and so retained relatively low abundances of

HSE. Subsequent dynamical models have highlighted the probability that bodies of similar mass may have survived beyond the formation age of the Moon, and thus been available to participate in stochastic late accretion (Marchi et al., 2014). Bottke et al. (2010) reported that for impactors with diameters between 2000 and 2500 km, slightly more than 10% of their dynamical simulations could achieve the necessary relative enrichments in HSE to the mantles of the Earth, Moon and Mars.

If stochastic late accretion correctly accounts for the apparent disparity in HSE abundances between the lunar and terrestrial mantles, it has a major implication for tracing late stage building blocks of the Earth, and possibly Mars. It requires that mass was added to the Earth by a limited number of impact events that likely would have generated discrete magma seas or lakes, rather than as a chemically and isotopically well-mixed veneer of small bodies. Consequently, if late stage impactors were added to the mantle in such a way that global melting did not occur, then the impactors may have imparted isotopically distinct HSE signatures to different portions of the mantle, assuming the impactors were genetically different from the average BSE, and from one another.

But what is the likelihood that moderately-sized, early-formed mantle heterogeneities remained isotopically distinct for hundreds of millions of years, until they melted to produce rocks that became incorporated into the rock record? This is where it is important to consider data for the short-lived radiogenic isotope systems. Perhaps of greatest importance for consideration here are $\mu^{182}W$ isotopic data for rocks that were ultimately derived from the terrestrial mantle. Anomalous $\mu^{182}W$ values have been identified in a number of ancient rocks, including ≥3.8 Ga supracrustal rocks from Nuvvuagittuq, Quebec (Touboul et al., 2014), ~3.7 Ga supracrustal rocks from Isua, Greenland (Willbold et al., 2011), and 2.8 Ga komatiites from

668 Kostomuksha, Fennoscandia (Touboul et al., 2012). All ^{182}W anomalies for terrestrial rocks,
669 reported to date, range between +5 and +15 ppm (**Fig. 10**). These terrestrial anomalies are much
670 smaller than the isotopic variations that have been observed for other early solar system objects,
671 which range from initial μ^{182}W values determined for calcium aluminum-rich inclusions of ~-
672 350 ppm, to enriched values of as much as +4000 ppm in some eucrites (Kleine et al., 2009).
673 Terrestrial enrichments in ^{182}W have been interpreted in two different ways. Willbold et al.
674 (2011) reported ^{182}W enrichments averaging ~13 ppm for 3.7 Ga supracrustal rocks from Isua,
675 Greenland. These authors proposed that the enriched compositions reflect derivation of precursor
676 rocks from a mantle domain that formed prior to a final major stage of late accretion, and that
677 this mantle domain remained mostly free of late accreted materials until it melted to form the
678 Isua rocks. Thus, the mantle precursor materials to the Isua rocks formed by normal planetary
679 accretion, were stripped of HSE by metal segregation during core formation, then remained
680 isolated from HSE and W (with low μ^{182}W) added by subsequent late accretion. This is a process
681 that could lead to isotopic heterogeneity in the mantle long after ^{182}Hf became extinct. Most
682 importantly, this mantle domain was not contaminated with late accreted HSE as a result of
683 mantle mixing until after the early Archean melting event that produced the Isua precursor rocks,
684 presumably well after completion of the dominant phase of late accretion. This requires
685 inefficient mixing of the mantle during the Hadean through early Archean. If this interpretation
686 is correct for the Isua rocks, then the mantle domain sampled by them should have been
687 relatively devoid of HSE. Willbold et al. (2011), however, did not report complementary HSE
688 for these rocks. Even when this is eventually done, however, it should be recognized that
689 constraining the concentrations of HSE in the mantle source(s) of such highly altered
690 supracrustal rocks will be challenging.

691 A second means to account for anomalous ^{182}W in mantle-derived rocks is by solid-liquid
692 fractionation processes that may have occurred in the mantle while ^{182}Hf was still extant.
693 Because the absolute HSE abundances estimated for the mantle source of the Kostomuksha
694 komatiites are nearly identical, within uncertainties (Puchtel and Humayun, 2005), to those in the
695 BSE estimates of Becker et al. (2006), Touboul et al. (2012) rejected the model of Willbold et al.
696 (2011) for these rocks. They instead concluded that either metal-silicate fractionation in a basal
697 magma ocean, or silicate crystal-liquid fractionation in a more conventional, whole mantle
698 magma ocean led to the creation of a mantle domain characterized by high Hf/W. This in turn led
699 to the formation of a domain that evolved to high $\mu^{182}W$, as ^{182}Hf decayed. Because of the short
700 lifetime of ^{182}Hf, it was concluded that the fractionation events occurred within the first 30 Myr
701 of solar system history. Similar processes may also have led to the creation of some ^{142}Nd
702 anomalies (e.g., Brown et al., 2014).
703 Regardless of the true mechanisms involved in the generation of terrestrial ^{182}W anomalies,
704 it is clear that their presence in the rock record requires the long term survival of chemical
705 heterogeneities in the terrestrial mantle, despite presumably vigorous convective mixing. Much
706 larger ^{182}W and ^{142}Nd isotopic anomalies have been determined for some, but not all martian
707 meteorites, so the martian mantle also likely escaped a final large-scale homogenization event
708 during the final stages of its growth. Thus, if these bodies experienced late stages of accretion
709 from genetically diverse materials, it might be expected that attenuated signals from the various
710 materials might be summoned from the rock record. Limited high precision analyses of Ru
711 isotopes in terrestrial materials have, as yet, not identified any isotopic heterogeneity within the
712 mantle (Bermingham et al., 2015), but the search has just begun.
713

714

715 *5.3. The Mo-Ru Connection*

716 In the discussion above, it is noted that the Mo and Ru present in the mantle today were
717 most likely emplaced by different late-stage accretionary processes. The Mo abundance of the
718 mantle was dominantly established by the final ~10-20 % of terrestrial accretion, with major
719 input from the giant impact stage of growth, culminating in the Moon-forming giant impact. The
720 Mo isotopic composition of the mantle probably represents a mixture of Mo from the silicate
721 portion of the proto-Earth, as well as Mo from both the core and mantle of the giant impactor. By
722 contrast, most Ru was likely added to the mantle by late accretion. Dauphas et al. (2004; 2014)
723 made the important observation that, when plotting the range of nucleosynthetic heterogeneities
724 for Mo and Ru in bulk planetary materials, most of these materials plot along a generally linear
725 trend, with the Earth, IAB irons, and enstatite chondrites plotting at one end, and some
726 carbonaceous chondrites plotting at the other end of the trend (**Fig. 11**). Based on this
727 correlation, these authors surmised that because each element recorded the genetics of different,
728 late-stages of terrestrial accretion, it is logical to conclude that the materials involved in both
729 stages were genetically related, and may have been derived from roughly the same portion of the
730 protoplanetary disk. Thus, there may have been no major change in the genetic make-up of
731 materials involved in the Moon-forming giant impact as compared to the final ~0.5% of late
732 accreted materials (Dauphas et al., 2004; 2014). Differing genetics of these additions would
733 otherwise have led to Earth plotting off of this correlation. As discussed above, this observation
734 can also be extended back to the major portion of terrestrial accretion, given the enstatite
735 chondrite-like nature of both lithophile and siderophile elements.

736 This seemingly does not bode well for identifying genetically diverse materials in the
737 mantle. However, Mo and Ru isotope data underpinning this important observation remain
738 limited. The correlation is presently constructed using group averages determined for a limited
739 number of meteorites for which the Mo and Ru isotope compositions are not obtained from the
740 same pieces of meteorite. Consequently, the precise relationship between Mo-Ru in different
741 meteorites needs to be clarified using high precision Mo and Ru isotope composition data
742 obtained from the same meteorite pieces.
743
744 In summary, the relatively high, and chondrite-like relative abundances of HSE in the
745 terrestrial mantle are best explained by their addition via late accretion of ~0.5 wt. % of Earth's
746 mass to the mantle following cessation of core formation. The similar absolute and relative
747 abundances of HSE estimated for the martian mantle, and the much lower abundances of HSE in
748 the lunar mantle, however, are problematic for late accretionary models. One way to account for
749 these observations is by stochastic late accretion, whereby late accretionary mass to the Earth
750 and Mars was primarily added through the impact of several 10^{22} kg mass objects, whereas the
751 Moon was not struck by such large impactors.
752 The HSE characteristics of the BSE, as assessed by the relative abundances of the HSE
753 (including $^{187}Os/^{188}Os$) are most like enstatite and ordinary chondrites, although the HSE
754 characteristics of the BSE are not a perfect match to any chondrite group. Osmium isotopes
755 strongly suggest that the late accreted materials to Earth were not like carbonaceous chondrites.
756 Although still very limited for both terrestrial rocks and meteorites, Ru isotopic composition data
757 are also consistent with a dominant late accretionary component to the Earth that is genetically
758 similar to enstatite chondrites. Remarkably, this may indicate that the genetic make-up of even

late-accreted materials to Earth, did not diverge substantially from the basic building blocks of the Earth.

6. Late Heavy Bombardment: The final ~≤0.05 wt. % of Accretion?

It has long been hypothesized that the Earth-Moon system, and likely the entire inner solar system, underwent a phase of late accretion, termed *late heavy bombardment* (LHB), within the interval from ~4.1 to ~3.8 Ga. The evidence for this putative event primarily comes from geochronologic information obtained from a variety of shocked and/or melted lunar rocks (e.g., Turner et al., 1973; Tera et al., 1974; Kring and Cohen, 2002). For example, Tera et al. (1974) recognized that most rocks collected by the Apollo missions formed a linear trend on a plot of $^{207}Pb/^{206}Pb$ versus $^{238}U/^{204}Pb$ that intersects concordia at about 3.9 Ga. Because of the ubiquity of this age, they inferred that the Moon underwent what they referred to as a *terminal cataclysm*. They envisioned the cataclysm to have been a relatively brief period of heavy bombardment (<300 million years) during which the surface of the Moon, and presumably the Earth, was peppered with large impactors, leading to the creation of at least some of the lunar basins. Current estimates suggest the basin-forming impactors were as large as 200 km in diameter (e.g., Hurwitz and Kring, 2014). Subsequent studies of lunar impact melt rocks have provided strong support for a major disturbance in ages at about 3.9 Ga (e.g. Dalrymple and Ryder, 1993; Cohen et al., 2000), as few impact-modified lunar rocks yield ages older than ~3.9 Ga. Although the LHB had a major effect on shaping the surface of the Moon, it likely involved much less mass than is envisioned for late accretion as a whole. Even generous estimates for the mass of the LHB, based on assumptions about the masses of basin-forming impactors, place the mass of materials involved at no more than about 10% of estimates for the overall mass of late

782 accretionary additions (0.05 wt.% accretion)(e.g., Morgan et al., 2001), and some dynamical
783 models suggest that only about 1% (0.005 wt.% accretion) was added by the LHB (Marchi et al
784 2014; Morbidelli et al. 2012).

785 Dynamical models for the evolution of the solar system have suggested some possible
786 causes for a period of LHB (Morbidelli et al., 2001; Strom et al., 2005; Gomes et al., 2005;
787 Chambers, 2007). For example, Gomes et al. (2005) suggested that migration of Uranus and
788 Neptune, resulting from Jupiter and Saturn entering a 2 to 1 orbital resonance, may have led to
789 the perturbation in the orbits of small bodies from both the asteroid belt and the Kuiper belt.
790 Chambers (2007) suggested that the removal of a now missing additional planet, between the
791 orbit of Mars and the asteroid belt, could have triggered the LHB. Despite these observations and
792 models, it is also possible that the ~3.9 Ga age represents a re-set age for the samples from a
793 limited areal extent on the near-side of the Moon, from which all Apollo samples were collected,
794 or even sampling of ejecta from only the youngest of the major basins (Spudis et al., 2011).

795 In addition to seeking to understand the timing of the LHB, it is also imperative to
796 constrain the chemical characteristics of the materials involved in the bombardment because of
797 the possibility that they delivered substantial water and other volatile species to the Earth and
798 Moon. The primary means to examine the chemical characteristics of materials from the putative
799 LHB has been to analyze lunar impact melt rocks that were created as a result of the basin-
800 forming impacts. Such studies have been pursued since the Apollo missions, with chemical
801 characterizations focused upon siderophile elements (e.g., Morgan et al., 1972; 1974; Korotev,
802 1994). Siderophile element data for nearly all studies prior to ca. 2000 were obtained by neutron
803 activation analysis, so elements such as Ir, Au, Ni and Ge, that can be well-measured by this
804 method, were most commonly considered. For example, Morgan et al. (1974) concluded that

805 rocks from the Apollo 17 site included meteoritic components from at least six impactors, none
806 of which had siderophile element characteristics that perfectly matched known meteorites.
807 Such studies as Morgan et al. (1974) assumed that endogenous lunar highlands or basaltic
808 rocks formed with very low siderophile element abundances, so that the siderophile elements
809 present in the impact melt rocks were nearly entirely derived from one or more large impactors.
810 A substantial number of studies reporting siderophile element data for so-called pristine lunar
811 rocks have generally borne out this assumption (e.g., Warren and Wasson, 1977; Ryder et al.,
812 1980; Warren et al., 1991; Day et al., 2007; 2010).
813 Although the early studies provided highly valuable insights into the chemical nature of
814 impactors, some of the chief elements used to discriminate among possible impactors, such as
815 Au and Ge, are moderately volatile and could potentially have been modified by high
816 temperature impact processes. To circumvent this problem, Norman et al. (2002) first applied the
817 isotope dilution technique, teamed with inductively-coupled plasma mass spectrometry, to
818 measure a larger suite of HSE in Apollo 17 impact melt rocks. That study measured and reported
819 data for Re, Ir, Ru, Pt, and Pd, and identified at least three sources of HSE to the Apollo 17 suite.
820 One source had HSE ratios similar to ordinary chondrites. A second component was
821 characterized by HSE similar to EH chondrites. In order to account for suprachondritic Re/Ir,
822 Ru/Ir, and Pd/Ir in most of the rocks, Norman et al. (2002) appealed to the possibility of a third
823 component, either an endogenous component enriched in Re, Ru and Pd, or an older component
824 in the target crust that was incorporated into the crust by an earlier impactor with non-chondritic
825 relative abundances of HSE.
826 Four recent, subsequent studies have utilized similar isotope dilution techniques to measure
827 the abundances of Re, Os, Ir, Ru, Pt, and Pd in lunar impact melt rocks, as well as measure

828 $^{187}Os/^{188}Os$, which serves as a sensitive proxy for long-term Re/Os (Puchtel et al., 2008; Fischer-
829 Gödde and Becker, 2012; Sharp et al., 2014; Liu et al., 2015). A major difference between these
830 studies and the study of Norman et al. (2002) is that they examined multiple pieces of each rock
831 studied. In approximately half of the rocks examined, the resulting plots of Ir versus each of the
832 other HSE measured yielded linear trends with intercepts indistinguishable from 0, within
833 regression uncertainties (**Fig 12**). In such cases, the trends can be assumed to represent mixing
834 between the exogenous impactor and the HSE poor lunar target rocks, similar to interpretations
835 for terrestrial impact melt rocks (e.g., McDonald et al., 2001). The slopes of the linear trends can,
836 therefore, be assumed to record the HSE ratios of the basin forming impactors.
837 Puchtel et al. (2008) and Sharp et al. (2014) reported and interpreted data mainly for Apollo
838 17 impact melt rocks. Both studies reported a "dominant" component for the site, most notably
839 characterized by suprachondritic Re/Os (as measured by $^{187}Os/^{188}Os$), as well as Ru/Ir and Pd/Ir
840 comparable to the results from Norman et al. (2002). They interpreted the results to suggest that
841 the dominant source of HSE to the site, most likely the spatially associated Serenitatis basin
842 impactor, shared broad similarities to some chondritic meteorites (enstatite chondrites), but
843 sampling a composition not presently found in our meteorite collections. By contrast, a feldspar
844 rich, or *granulitic* component present as clasts in some of these rocks, was determined to be
845 characterized by relative abundances of HSE more similar to carbonaceous and ordinary
846 chondrites.
847 Fischer-Gödde and Becker (2012) focused mainly on impact melt rocks from the Apollo 16
848 site. Here, they found Re/Os, Ru/Ir, Pt/Ir, and Pd/Ir ratios extending much higher than in known
849 chondrites, and even well beyond the range of Apollo 17 rocks. They also analyzed some
850 granulitic rocks and reported that, like prior studies, this component is most like ordinary

851 chondrites. Of note, this study recognized that virtually all of the HSE data for Apollo samples
852 plot along linear trends of HSE/Ir versus $^{187}Os/^{188}Os$. They interpreted this to mean that all of the
853 Apollo impact melt rocks incorporated at least two HSE-rich components at the time of their
854 formation. One was very similar to carbonaceous chondrites and is the major component in
855 granulitic rocks. The other component resembles a chemically evolved group IVA iron
856 meteorite. Consequently, they proposed that both components became variably mixed during
857 basin-forming impacts, but were not substantially modified by the inclusion of HSE derived from
858 the basin-forming impactors.

859 Most recently, data from Liu et al. (2015) for Apollo 15 and 16 melt rocks filled in the gaps
860 in the apparent linear trend recognized by Fischer-Gödde and Becker (2012), thus, strengthening
861 their observation. In the compilation of data reported by Liu et al. (2015), nearly all data for
862 lunar impact melt rocks plot along a continuous linear trend ranging from a HSE composition
863 that is broadly chondritic, to an endmember with $^{187}Os/^{188}Os$, Ru/Ir and Pd/Ir ratios far above
864 those of known chondrites (**Fig. 13**). Two possible scenarios to explain the observed trends are:
865 1) Variable mixing between an earlier granulitic contaminant and a series of later-stage
866 impactors that happened to form co-linear, suprachondritic Re/Os, Ru/Ir, Pt/Ir and Pd/Ir. 2)
867 Variable mixing between two components present in the lunar crust prior to the late-stage basin
868 forming impacts. For this scenario, one component was chondritic in composition and the other
869 component had fractionated HSE, and could have been a core fragment, as suggested by Fischer-
870 Gödde and Becker (2012). Although the latter scenario requires the involvement of a portion of
871 an evolved core, it currently appears to be the most simplistic explanation for the trend. It also
872 requires that the later-stage basin forming impacts (e.g., Imbrium) added only very limited HSE

873 to the sampled impact melt rocks from multiple sites. These models await genetic testing using
874 the nucleosynthetic anomalies characteristic of siderophile elements Mo and Ru.
875
876 In summary, the HSE characteristics of lunar impact melt rocks, believed to have formed as
877 a result of basin forming events during a possible LHB, include at least two major components.
878 One, with HSE characteristics similar to carbonaceous or ordinary chondrites, the other
879 component is much more highly fractionated and most resembles a portion of a core represented
880 by some iron meteorites. One way to account for the data is to conclude that both components
881 were incorporated in the lunar crust prior to the LHB, and that the basin-forming impacts mainly
882 resulted in variable mixing of the older components. No isotopic data, e.g., Ru, are as yet
883 available for genetic testing of these components.
884
885
886 **7. Putting It All Together**
887 At the present time, combined lithophile and siderophile element data suggest that the
888 primary building blocks of Earth were isotopically broadly similar to enstatite chondrites, but
889 probably substantially differed from enstatite chondrites in terms of major element composition.
890 Combining isotopic data for lithophile and siderophile elements that serve as genetic tracers
891 leads to the suggestion that there was not a major change in the provenance of building blocks
892 when comparing the pre-giant impact Earth, to the inferred composition of the Moon-forming
893 giant impactor. This conclusion is based on the reasoning that the isotopic similarities between
894 the Earth and enstatite chondrites, for lithophile elements such as O and Cr, indicate genetic
895 similarity to enstatite chondrites prior to the giant impact. Yet, the isotopic composition of the

siderophile element Mo in Earth's mantle is also very similar to that of enstatite chondrites. The isotopic composition of Mo present in the mantle was likely strongly affected by additions from the Moon-forming giant impactor, whereas the isotopic compositions of lithophile elements such as O and Cr were not. Thus, the collective enstatite chondrite-like isotopic compositions of lithophile and siderophile elements suggest that both the Earth and the giant impactor formed in the same region of the protoplanetary disk as enstatite chondrites (e.g., Dauphas et al., 2014).

The genetic heritage of late accreted materials during the final 0.5 wt. % of terrestrial accretion is best monitored via Ru isotopes, combined with the relative abundances of the HSE in the BSE. The Ru isotopic composition of the mantle (Bermingham et al., 2015), as for Mo isotopes, is similar to enstatite chondrites, meaning that the Earth plots near enstatite chondrites at the end of the cosmic Ru-Mo correlation trend. Some aspects of the projected relative abundances of the HSE in the BSE also match certain enstatite chondrites (Pd/Ir and $^{187}Os/^{188}Os$). However, other aspects of the HSE signature of the BSE, such as Ru/Ir, do not match any known chondrite groups. Thus, the late accreted materials must include at least one component with more fractionated HSE than is known to occur in chondrites. The origin of this chemical signature remains poorly constrained, but is suggestive of a not yet sampled primitive meteorite component. Very limited Os isotopic data for Mars suggest a similar late accretionary component was added to its mantle.

Finally, the Earth and Moon were bombarded by an additional flux of planetesimals hundreds of millions of years after primary accretion. The accretionary additions associated with this period could have totaled as much as 0.05 wt. % of the mass of the Earth. The materials involved in this final, minor accretionary period also involved the addition of HSE with some fractionated ratios. The chemical and isotopic natures of these materials are best monitored

through the analysis of lunar impact melt rocks that were created by the late-stage basin-forming events. The fingerprints of these impactors are complex and encompass a range of HSE compositions. Some components evident in this bombardment cohort appear to be similar in HSE characteristics to carbonaceous and ordinary chondrites. An additional component was characterized by substantially higher Re/Os, Ru/Ir and Pd/Ir, compared to any known chondrites, including enstatite chondrites. The dominant signature of at least some materials involved in the LHB, therefore, appear distinct from the prior late-stage building blocks. The Ru and Mo isotopic compositions of lunar impact melt rocks have not yet been determined, so it remains unknown whether or not the LHB can be genetically linked to a type of primitive meteorite.

Although the siderophile element data for the Earth suggest that there was no major change in the provenance of its building blocks through to the end of late accretion (but before LHB), it remains unknown whether or not the building blocks consisted of a genetically homogeneous flux, or included diverse materials that ultimately mixed to form what now appears to be a uniform fingerprint for the BSE. The possibility of isotopic variability of Ru and Mo among potential late stage building blocks, combined with the apparent sluggishness of early mantle mixing of primordial ^{182}W isotopic heterogeneities, suggests that isotopic evidence for diverse late stage impactors might be found in Earth's early rock record, and possibly in younger rocks. Conversely, given the high level of precision that is now available to search for such isotopic heterogeneities, the future lack of discovery of isotopic anomalies may signal either that the materials involved in the final stages of terrestrial accretion were genetically similar, or that early mixing processes attenuated early Earth heterogeneities before evidence for them could be incorporated in the surviving rock record.

Acknowledgements

This work has been supported by NASA grants NNX13AF83G and NNA14AB07A, and NSF-CSEDI grants EAR1160728 and EAR1265169. These sources of funding are gratefully acknowledged. RJW also thanks the University of Maryland for providing sabbatical support, as well as the Carnegie Institution of Science's Department of Terrestrial Magnetism, the Lunar and Planetary Institute, and the Tokyo Institute of Technology's Earth-Life Science Institute for hosting him during the writing of this paper. David Rubie and an unidentified reviewer are thanked for providing very thorough and helpful criticisms of the original manuscript.

950 **References**

951

952 Alard, O., Griffin W.L., Lorand, J.-P., Jackson, S.E., O'Reilly, S.Y., 2000. Non-chondritic
953 distribution of the highly siderophile elements in mantle sulphides. Nature 407, 891-894.
954 Albarede, F., Ballhaus, C., Blichert-Toft, J., Lee, C.-T., Marty, B., Moynier, F., Yin, Q.-Z., 2013.
955 Asteroidal impacts and the origin of terrestrial and lunar volatiles. Icarus 222, 44–52.
956 Anders, E., 1968. Chemical processes in the early Solar System, as inferred from meteorites.
957 Acc. Chem. Res. 1, 289-298.
958 Anders, E., Grevesse, N., 1989. Abundances of the elements: meteoritic and solar. Geochim.
959 Cosmochim. Acta 53, 197-214.
960 Andreasen, R., Sharma, M., 2007. Mixing and homogenization in the early Solar System: clues
961 from Sr, Ba, Nd, and Sm isotopes in meteorites. Astrophys. Journ. 665, 874-883.
962 Archer, G.J., Bullock, E.S., Ash, R.D., Walker, R.J., 2014. ^{187}Re-^{187}Os isotopic and highly
963 siderophile element systematics of the Allende meteorite: evidence for primary nebular
964 processes and late-stage alteration. Geochim. Cosmochim. Acta 131, 402-414.
965 Azbel, I.Y., Tolstikhin, I.N., Kramers, J.D., Pechernikova, G.V., Vityazev, A.V., 1993. Core
966 growth and siderophile element depletion of the mantle during homogeneous Earth accretion.
967 Geochim. Cosmochim. Acta 57, 2889-2898.
968 Balsiger, H., Altwegg, K., Geiss, J., 1995. D/H and $^{18}O/^{16}O$ ratio in the hydronium ion and in
969 neutral water from in situ ion measurements in Comet Halley. J. Geophys. Res. 100, 5827-
970 5834.
971 Barnes, S.-J., Naldrett, A.J., Gorton, M.P., 1985. The origin of the fractionation of plantinum-
972 group elements in terrestrial magmas. Chem. Geol. 53, 303-323.

973 Becker, H., Horan, M.F., Walker, R.J., Gao, S., Lorand, J.-P., Rudnick, R.L., 2006. Highly
974 siderophile element composition of the Earth's primitive upper mantle: Constraints from
975 new data on peridotite massifs and xenoliths. Geochim. Cosmochim. Acta 70, 4528-4550.
976 Bermingham, K.R., Walker, R.J., Worsham, E.A., 2015. Refinement of the Mo-Ru isotope
977 cosmic correlation using high precision Mo and Ru isotope data. Lunar and Planet. Sci.
978 Conf. 46, abstract # 1588.
979 Bizzarro, M., Ulfbeck, D., Trinquier, A., Thrane, K., Connelly, J.N., Meyer, B.S., 2007.
980 Evidence for a late supernova injection of ^{60}Fe into the protoplanetary disk. Science 316,
981 1178–1181.
982 Borisov, A., Palme, H., Spettel B., 1994. Solubility of palladium in silicate melts: implications
983 for core formation in the Earth. Geochim. Cosmochim. Acta 58, 705-716.
984 Bottke, W.F., Walker, R.J., Day, J.M.D., Nesvorny, D., Elkins-Tanton, L., 2010. Stochastic late
985 accretion to Earth, the Moon and Mars. Science 330, 1527-1530.
986 Boyet, M., Carlson, R.W., 2005. ^{142}Nd evidence for early (>4.53 Ga) global differentiation of the
987 silicate Earth. Science 309, 576-581.
988 Brandon, A.D., Humayun, M., Puchtel, I.S., Leya, I., Zolensky, M., 2005. Osmium isotope
989 evidence for an s-process carrier in primitive chondrites. Science 309, 1233-1236.
990 Brandon, A.D., Walker, R.J., Puchtel, I.S., 2006. Platinum-Os isotope evolution of the Earth's
991 mantle: constraints from chondrites and Os-rich alloys. Geochim. Cosmochim. Acta 70,
992 2093-2103.
993 Brandon, A.D., Puchtel, I.S., Walker, R.J., Day, J.M.D., Irving, A.J., Taylor, L.A., 2012.
994 Evolution of the martian mantle inferred from the ^{187}Re-^{187}Os isotope and highly

995 siderophile element systematics of shergottites meteorites. Geochim. Cosmochim. Acta76,
996 206-235.
997 Brenan, J.M., McDonough, W.F., 2009. Core formation and metal–silicate fractionation of
998 osmium and iridium from gold. Nature Geoscience 2, 798-801.
999 Brown, S., Elkins-Tanton, L., Walker, R.J., 2014. Effects of magma ocean crystallization and
1000 overturn on the development of ^{142}Nd and ^{182}W isotopic heterogeneities in the primordial
1001 mantle. Earth Planet. Sci. Lett. 408, 319-330.
1002 Burbidge, E.M., Burbidge, G.R., Fowler, W.A., Hoyle, F., 1957. Synthesis of the elements in
1003 stars. Rev. Mod. Phys. 59, 547-650.
1004 Burkhardt,C., Kleine, T., Oberli, F., Pack, A., Bourdon, B., Wieler, R., 2011. Molybdenum
1005 isotope anomalies in meteorites: Constraints on solar nebula evolution and origin of the
1006 Earth. Earth Planet. Sci. Lett. 312, 390-400.
1007 Campbell. I.H., Griffiths, R.W., Hill, R.I., 1989. Melting in an Archaean mantle plume: head it's
1008 basalts, tails it's komatiites. Nature 339, 697-699.
1009 Canup, R.M., Asphaug, E., 2001. Origin of the Moon in a giant impact near the end of the
1010 Earth's formation. Nature 412, 708-712.
1011 Canup, R.M., 2012. Forming a Moon with an Earth-like composition via a giant impact. Science
1012 338, 1052-1055.
1013 Carlson, R.W., Boyet, M., Horan, M., 2007. Chondrite barium, neodymium, and samarium
1014 isotopic heterogeneity and early earth differentiation. Science 316, 1175–1178.
1015 Caro, G., Bourdon, B., Birck, J.-L., Moorbath, S., 2003. ^{146}Sm–^{142}Nd evidence from Isua
1016 metamorphosed sediments for early differentiation of the Earth’s mantle. Nature 423, 428–
1017 432.

1018 Caro, G., Bourdon, B., Birck, J-L., Moorbath, S., 2006. High-precision $^{142}Nd/^{144}Nd$
1019 measurements in terrestrial rocks: constraints on the early differentiation of the Earth's
1020 mantle. Geochim. Cosmochim. Acta 70, 164–191.
1021 Chambers, J.E., 2001. Making more terrestrial planets, Icarus 152, 205– 224.
1022 Chambers, J.E., 2004. Planetary accretion in the inner Solar System. Earth Planet. Sci. Lett. 223,
1023 241–252.
1024 Chambers, J.E., 2007. On the stability of a planet between Mars and the asteroid belt:
1025 Implications for the Planet V hypothesis. Icarus 189, 386-400.
1026 Chen, J.H., Papanastassiou, D.A.,Wasserburg, G.J., 2010. Ruthenium endemic isotope effects in
1027 chondrites and differentiated meteorites. Geochim. Cosmochim. Acta 74, 3851–3862.
1028 Chou, C.-L., 1978. Fractionation of siderophile elements in the Earth's upper mantle. Proc.
1029 Lunar Planet. Sci. Conf. 9th, 219-230.
1030 Clayton, R.N., Mayeda T.K., Rubin A.E., 1984. Oxygen isotopic compositions of enstatite
1031 chondrites and aubrites. Proc. Fifteenth Lunar Planet. Sci Conf., Part 1, Journ. Geophys.
1032 Res. 89, C245-249.
1033 Clayton, R.N., 2002. Self-shielding in the solar nebula. Nature 415, 860–861.
1034 Cohen, B.A., Swindle, T.D., Kring, D.A., 2000. Support for the lunar cataclysm hypothesis from
1035 lunar meteorite impact melt ages. Science 290, 1754-1756.
1036 Cottrell, E., Walker, D., 2006. Constraints on core formation from Pt partitioning in mafic
1037 silicate liquids at high temperatures. Geochim. Cosmochim. Acta 70, 1565-1580.
1038 Ćuk, M., Stewart S.T., 2012. Making the Moon from a fast-spinning Earth: a giant impact
1039 followed by resonant despinning. Science 338, 1047-1052.

1040 Dahl, T.W., Stevenson, D.J., 2010. Turbulent mixing of metal and silicate during planet
1041 accretion - and interpretation of the Hf–W chronometer. Earth Planet. Sci. Lett. 295, 177-
1042 186.
1043 Dalrymple, G.B., Ryder, G., 1993. $^{40}Ar/^{39}Ar$ age spectra of Apollo 15 impact melt rocks by laser
1044 step-heating and their bearing on the history of lunar basin formation. Journ. Geophys.
1045 Res. 98, 13,085-13,095.
1046 Dauphas, N. Marty, B., Reisberg, L., 2002a. Molybdenum nucleosynthetic dichotomy revealed
1047 in primitive meteorites, Astrophys. Journ. 569 (2002) L139– L142.
1048 Dauphas, N. Marty, B., Reisberg, L., 2002b. Molybdenum evidence for inherited planetary scale
1049 isotope heterogeneity of the protosolar nebula. Astrophys. Journ. 565, 640-644.
1050 Dauphas, N. Davis, A.M., Marty, B., Reisberg, L., 2004. The cosmic molybdenum–ruthenium
1051 isotope correlation. Earth Planet. Science Lett. 226, 465– 475.
1052 Dauphas, N., Pourmand, A., 2011. Hf–W–Th evidence for rapid growth of Mars and its status as
1053 a planetary embryo. Nature 473, 489–492.
1054 Dauphas, N., Burkhardt, C., Warren, P.H., Teng, F-Z., 2014. Geochemical arguments for an
1055 Earth-like Moon-forming impactor. Phil. Trans. Roy. Soc. A 372, 20130244.
1056 Day, J.M.D., Pearson, D.G., Taylor, L.A., 2007. Highly siderophile element constraints on
1057 accretion and differentiation of the Earth-Moon system. Science 315, 217-219.
1058 Day, J.M.D., Walker, R.J., James, O.B., Puchtel, I.S., 2010. Osmium isotope and highly
1059 siderophile element systematics of the lunar crust. Earth Planet. Sci. Lett. 289, 595-605.
1060 Debaille, V., Brandon, A.D., O'Neill, C., Yin, Q.-Z., Jacobsen, B., 2009. Early martian mantle
1061 overturn inferred from isotopic composition of nakhlite meteorites. Nature Geoscience 2,
1062 548-552.

1063 Debaille, V., O'Neill, C., Brandon, A.D., Haenecour, P., Yin, Q-Z., Mattielli, N., Treiman, A.H.,
1064 2013. Stagnant-lid tectonics in early Earth revealed by ^{142}Nd variations in late Archean
1065 rocks. Earth Planet. Sci. Lett. 373, 83-92.
1066 Drake, M.J., Righter, K., 2002. Determining the composition of the Earth. Nature 416, 39-44.
1067 Dwyer, C.A., Nimmo, F., Chambers, J.E., Bulk chemical and Hf–W isotopic consequences of
1068 incomplete accretion during planet formation. Icarus 245, 145-152.
1069 Eberhardt, P., Reber, M., Krankowsky, D., Hodges, R.R., 1995. The D/H and ^{18}O/^{16}O ratios in
1070 water from Comet P/Halley. Astron. Astrophys. 302, 301-316.
1071 Fischer-Gödde, M., Becker, H., Wombacher, F., 2010. Rhodium, gold and other highly
1072 siderophile element abundances in chondritic meteorites. Geochim. Cosmochim. Acta 74,
1073 356–379.
1074 Fischer-Gödde, M., Becker, H., Wombacher, F., 2011. Rhodium, gold and other highly
1075 siderophile elements in orogenic peridotites and peridotite xenoliths. Chem. Geol. 280,
1076 365–383
1077 Fischer-Gödde, M., Becker, H., 2012. Osmium isotope and highly siderophile element
1078 constraints on ages and nature of meteoritic components in ancient lunar impact rocks.
1079 Geochim. Cosmochim. Acta 77, 135–156.
1080 Fischer-Gödde, M., Kleine, T., Burkhardt, C., Dauphas, N. 2014. Origin of nucleosynthetic
1081 isotope anomalies in bulk meteorites: evidence from coupled Ru and Mo isotopes in acid
1082 leachates of chondrites. 45th Lunar Planet. Sci. Conf. (abst.), 2409.
1083 Fitoussi, C., Bourdon, B., 2012. Silicon isotope evidence against an enstatite chondrite Earth.
1084 Science 335, 1477-1480.

1085 Foley, C.N., Wadhwa, M., Borg, L.E., Janney, P.E., Hines, R., Grove, T.L., 2005. The early
1086 differentiation history of Mars from ^{182}W-^{142}Nd isotope systematics in the SNC meteorites.
1087 Geochim. Cosmochim. Acta 69, 4557-4571.
1088 Franchi, I.A., Wright, I.P., Sexton, A.S., Pillinger, C.T., 1999. The oxygen-isotopic composition
1089 of Earth and Mars. Meteorit. Planet. Sci. 34, 657-661.
1090 Frost, D.J., Liebske, C., Langenhorst, F., McCammon, C.A., Trønnes, R.G., Rubie D.C., 2004.
1091 Experimental evidence for the existence of iron-rich metal in the Earth's lower mantle.
1092 Nature 428, 409–412.
1093 Frost, D.J., McCammon, C.A., 2008. The redox state of Earth's mantle. Ann. Rev. Earth Planet.
1094 Sci. 36, 389–420.
1095 Goes, S., Spakman, W., Bijwaard, H., 1999. A lower mantle source for central European
1096 volcanism. Science 286, 1928–1931.
1097 Goldschmidt, V.J., 1937. The principles of distribution of chemical elements in minerals and
1098 rocks. Journ. Chem. Soc., 655-673
1099 Gomes, R., Levinson, H. F., Tsiganis, K., Morbidelli, A., 2005. Origin of the cataclysmic late
1100 heavy bombardment period of the terrestrial planets. Nature 435, 466-470.
1101 Halliday, A.N., 2004. Mixing, volatile loss and compositional change during impact-driven
1102 accretion of the Earth. Nature 427, 505-509.
1103 Halliday, A.N., 2008. A young Moon-forming giant impact at 70-110 million years accompanied
1104 by late-stage mixing, core formation and degassing of the Earth. Phil. Trans. Roy. Soc.
1105 London, Series A, 366, 4163-4181.
1106 Hartmann, W.K., Davis, D.R., 1975. Satellite-sized planetesimals and lunar origin. Icarus 24,
1107 504-515.

1108 Herwartz, D., Pack, A., Friedrichs, B., Bischoff, A., 2014. Identification of the giant impactor
1109 Theia in lunar rocks. Science 344, 1146-1150.
1110 Hidaka, H., Ohta, Y., Yoneda, S., 2003, Nucleosynthetic components of the early solar system
1111 inferred from Ba isotopic compositions in carbonaceous chondrites. Earth Planet. Sci. Lett.
1112 214, 455–466.
1113 Hillgren, V.J., Drake, M.J., Rubie, D.C., 1994. High pressure and temperature experiments on
1114 core-mantle segregation in the accreting Earth. Science 264, 1442–1445.
1115 Hirt, B., Herr, W., Hoffmeister W., 1963. Age determinations by the rhenium-osmium method.
1116 In: Radioactive Dating. International Atomic Energy Agency, Vienna, 35-43.
1117 Hofmann, A.W., 2003, Sampling mantle heterogeneity through oceanic basalts: isotopes and
1118 trace elements. 61-101. In: Carlson R.W. (ed.) *Treatise on Geochemistry*, vol. 2: The
1119 Mantle and Core, pp. 547–568. Elsevier, Oxford.
1120 Holzheid, A., Sylvester, P., O'Neill, H. St.C., Rubie, D.C., Palme, H., 2000. Evidence for a late
1121 chondritic veneer in the Earth's mantle from high-pressure partitioning of palladium and
1122 platinum. Nature 406, 396-399.
1123 Horan, M.F., Walker, R.J., Morgan, J.W., Grossman, J.N., Rubin, A., 2003. Highly siderophile
1124 elements in chondrites. Chem. Geol. 196, 5-20.
1125 Horan, M.F., Alexander, C.M.O'D.,Walker, R.J., 2009. Highly siderophile element evidence for
1126 early solar system processes in components from ordinary chondrites. Geochim.
1127 Cosmochim. Acta 73, 6984-6997.
1128 Hurwitz, D.M., Kring, D.A., 2014. Differentiation of the South Pole-Aitken basin impact melt
1129 sheet: Implications for lunar exploration. Journ. Geophys. Res.-Planets 119, 1110-1133.

1130 Jacobson, S.A., Morbidelli, A., Raymond, S.N., O'Brien, D.P., Walsh, K.J., Rubie, D.C., 2014.
1131 Highly siderophile elements in Earth's mantle as a clock for the Moon-forming impact.
1132 Nature 508, 84-87.
1133 Javoy, M., et al. (2010) The Chemical composition of the Earth: enstatite chondrite model, Earth
1134 Planetary Sci. Lett., 293, 259–268.
1135 Kerridge, J. F. 1985. Carbon, hydrogen and nitrogen in carbonaceous chondrites: Abundances
1136 and isotopic compositions in bulk samples. Geochim. Cosmochim. Acta 49, 1707-1714.
1137 Kimura, K., Lewis, R.S., Anders, E., 1974. Distribution of gold and rhenium between nickel-iron
1138 and silicate melts. Geochim. Cosmochim. Acta 38, 683-781.
1139 Kleine, T., Touboul, M., Bourdon, B., Nimmo, F., Mezger, K., Palme, H., Jacobsen, S.B., Yin,
1140 Q-Z., Halliday, A.N., 2009. Hf–W chronology of the accretion and early evolution of
1141 asteroids and terrestrial planets. Geochim. Cosmochim. Acta 73, 5150–5188.
1142 Kokuba, E., Uda, S. 1998. Oligarchic growth of protoplanets. Icarus 131, 171-178.
1143 Kortev, R., 1994. Compositional variation in Apollo 16 impact-melt breccias and inferences for
1144 the geology and bombardment history of the Central Highlands of the Moon. Geochim.
1145 Cosmochim. Acta 58, 3931-3969.
1146 Kramers, J.D., 1998. Reconciling siderophile element data in the Earth and Moon, W isotopes
1147 and the upper lunar age limit in a simple model of homogeneous accretion. Chem. Geol. 145,
1148 461-478.
1149 Kring, D.A., Cohen, B.A., 2002. Cataclysmic bombardment throughout the inner solar system
1150 3.9–4.0 Ga. Journ. Geophys. Res. 107, 10.1029/2001JE001529.
1151 Kruijer, T.S., Kleine, T., Fischer-Gödde, M., Sprung, P., 2015. Lunar tungsten isotopic evidence
1152 for the late veneer. Nature 520, 534-537.

1153 Le Roux, V., Bodinier, J.-L., Tommasi, A., Alard, O., Dautria, J.-M., Vauchez, A., Riches,
1154 A.J.V., 2007. The Lherz spinel lherzolite: Refertilized rather than pristine mantle. Earth
1155 Planet. Sci. Lett. 259, 599-612.
1156 Li, J., Agee, C.B., 1996. Geochemistry of mantle-core differentiation at high pressure. Nature
1157 381, 686-689.
1158 Li, J., Agee, C.B., 1996. The effect of pressure, temperature, oxygen fugacity and composition
1159 on partitioning of nickel and cobalt between liquid Fe-Ni-S alloy and liquid silicate:
1160 implications for the Earth's core formation. Geochim. Cosmochim. Acta 65, 1821–1832.
1161 Liu, J., Sharp, M., Ash R.D., Kring, D.A., Walker, R.J., 2015. Diverse impactors in Apollo 15
1162 and 16 impact melt rocks: evidence from osmium isotopes and highly siderophile elements.
1163 Geochim. Cosmochim. Acta 155, 122-153.
1164 Lorand, J.-P., Alard, O., Godard, M., 2009. Platinum-group element signature of the primitive
1165 mantle rejuvenated by melt-rock reactions: evidence from Sumail peridotites (Oman
1166 Ophiolite). Terra Nova 21, 35–40.
1167 Lyons, J.R., Young, E.D., 2005. CO self-shielding as the origin of oxygen isotope anomalies in
1168 the early solar nebula. Nature 435, 317-320.
1169 Maier, W.D., Barnes, S.J., Campbell, I.H., Fiorentini, M.L., Peltonen, P., Barnes, S.-J., Smithies,
1170 R.H., 2009. Progressive mixing of meteoritic veneer into the early Earth's deep mantle.
1171 Nature 460, 620-623.
1172 Mann, U., Frost, D.J., Rubie, D.C., 2009. Evidence for high-pressure core-mantle differentiation
1173 from the metal-silicate partitioning of lithophile and weakly-siderophile elements.
1174 Geochim. Cosmochim. Acta 73, 7360–7386.

Mann, U., Frost, D.J., Rubie, D.C., Becker, H., Audétat, A., 2012. Partitioning of Ru, Rh, Pd, Re, Ir and Pt between liquid metal and silicate at high pressures and high temperatures - implications for the origin of highly siderophile element concentrations in the Earth's mantle. Geochim. Cosmochim. Acta 85, 593-615.

Marchi, S., Bottke, W.F., Elkins-Tanton, L.T., Bierhaus, M., Wuennemnn, K., Morbidelli, A., Kring, D.A., 2014. Widespread mixing and burial of Earth's Hadean crust by asteroid impacts. Nature 511, 578-582.

Mason, B., Taylor, S.R., 1982. Inclusions in the Allende meteorite. Smithson. Contrib. Earth Sci. 25, 1–30.

McDonald, I., Andreoli, M.A.G., Hart, R.J., Tredoux, M., 2001. Platinum-group elements in the Morokweng impact structure, South Africa: evidence for the impact of a large ordinary chondrite projectile at the Jurassic–Cretaceous boundary. Geochim. Cosmochim. Acta 65, 299–309.

McDonough, W.F., Sun, S-s., 1995. The composition of the Earth. Chem. Geol. 120, 223-253.

McDonough, W.F., 2003. Compositional Model for the Earth's Core. In: Carlson R.W. (ed.) *Treatise on Geochemistry*, vol. 2: The Mantle and Core, pp. 547–568. Elsevier, Oxford.

McLeod, C.L., Brandon, A.D., Armytage, R.M.G., 2014. Constraints on the formation age and evolution of the Moon from ^{142}Nd–^{143}Nd systematics of Apollo 12 basalts. Earth Planet. Sci. Lett. 396, 179-189.

Meisel, T., Walker, R.J., Morgan, J.W., 1996. The osmium isotopic composition of the primitive upper mantle, Nature 383, 517-520.

Meisel, T., Walker, R.J., Irving, A.J., Lorand, J.-P., 2001. Osmium isotopic compositions of mantle xenoliths: a global perspective. Geochim. Cosmochim Acta. 65, 1311-1323.

1198 Morbidelli, A., Petit, J.-M., Gladman, B., Chambers, J., 2001. A plausible cause of the late heavy
1199 bombardment. Met. Planet. Sci. 36, 371-380.
1200 Morbidelli, A., Lunine, J.I., O'Brien, D.P., Raymond, S.N., Walsh, K.J., 2012. Building
1201 Terrestrial Planets. Ann. Rev. Earth Planet. Sci. Lett. 40, 251–275.
1202 Morbidelli, A., Wood, B., 2015. Late accretion and the late veneer. In: Gerald Schubert (editor-
1203 in-chief) *Treatise on Geophysics*, 2nd edition, Oxford: Elsevier, pp. xx-xx.
1204 Morgan, J.W., Laul, J.C., Kränenbühl, U., Ganapathy, R., Anders, E., 1972. Major impacts on
1205 the moon: characterization from trace elements in Apollo 12 and 14 samples. Proc. Third
1206 Lunar Sci. Conf., Supplement 3, Geochim. Cosmochim. Acta 2, 1377-1395.
1207 Morgan, J.W., Ganapathy, R., Higuchi, H., Kränenbühl, U., Anders, E., 1974. Lunar basins:
1208 tentative characterization of projectiles, from meteoritic elements in Apollo 17 boulders.
1209 Proc. Fifth Lunar Sci. Conf., Supplement 5, Geochim. Cosmochim. Acta 2, 1703-1736.
1210 Morgan, J.W., 1985. Osmium isotope constraints on Earth's late accretionary history. Nature
1211 317, 703-705.
1212 Morgan, J.W., 1986. Ultramafic xenoliths: clues to Earth's late accretionary history. J. Geophys.
1213 Res. 91, 12,375-12,387.
1214 Morgan, J.W., Walker, R.J., Brandon, A.D., Horan, M.F., 2001. Siderophile elements in Earth's
1215 upper mantle and lunar breccias: Data synthesis suggests manifestations of the same late
1216 influx. Met. Planet. Sci. 36, 1257-1275.
1217 Mukhopadhyay, S., 2012. Early differentiation and volatile accretion recorded in deep-mantle
1218 neon and xenon. Nature 486, 101-106.
1219 Murthy, V., 1991. Early differentiation of the Earth and the problem of mantle siderophile
1220 elements; a new approach. Science 253, 303-306.

1221 Nimmo, F., O'Brien, D.P., Kleine, T., 2010. Tungsten isotopic evolution during late-stage
1222 accretion: Constraints on Earth–Moon equilibration. Earth Planet. Sci. Lett. 292, 363–370.
1223 Nittler, L.R., 2003. Presolar stardust in meteorites:recent advances and scientic frontiers. Earth
1224 Planet. Sci. Lett. 209, 259-273.
1225 Nolet, G., Karato, S.-I., Montelli, R., 2006. Plume fluxes from seismic tomography. Earth Planet.
1226 Sci. Lett. 248, 685-699.
1227 Norman, M. D., Bennett, V. C., Ryder, G., 2002. Targeting the impactors: siderophile element
1228 signatures of lunar impact melts from Serenitatis. Earth Planet. Sci. Lett. 202, 217–228.
1229 Nyquist, L.E., Wiesmann, H., Bansai, B.,Shih, C.-Y., Keith, J.E., Harper, C.L.,1995. ^{146}Sm–
1230 ^{142}Nd formation interval for the lunar mantle. Geochim. Cosmochim. Acta 59,2 817–2837.
1231 O'Brien, D.P., Walsh, K.J., Morbidelli, A., Raymond, S.N., Mandell, A.M., 2014. Water
1232 delivery and giant impacts in the 'Grand Tack' scenario. Icarus 239, 74–84.
1233 Pahlevan, K. and Stevenson, D.J., 2007. Equilibration in the aftermath of the lunar-forming giant
1234 impact. Earth Planet. Sci. Lett. 262, 438–449.
1235 Palme, H., O'Neill H.S.C., 2003. Cosmochemical estimates of mantle composition. In: H.D.
1236 Holland and K.K. Turekan (editors-in-chief) *Treatise on Geochemistry*, Oxford: Elsevier,
1237 volume 2, pp. 1-38.
1238 Pearson, D.G., Irvine, G.J., Ionov, D.A.., Boyd, F.R., Dreibus, G.E., 2004. Re–Os isotope
1239 systematics and platinum group element fractionation during mantle melt extraction: a
1240 study of massif and xenolith peridotite suites. Chem. Geol. 208, 29– 59
1241 Peucker-Ehrenbrink, B., Jahn, B.-m., 2001. Rhenium-osmium isotope systematics and platinum
1242 group element concentrations: loess and the upper continental crust. Geochem. Geophys.
1243 Geosyst. 2, 2001GC000172.

1244 Puchtel, I.S., Brandon, A.D., Humayun, M., 2004a. Precise Pt-Re-Os isotope systematics of the
1245 mantle from 2.7-Ga komatiites. Earth and Planetary Science Letters 224, 157-174.
1246 Puchtel, I.S., Humayun, M., Campbell, A., Sproule, R., Lesher, C.M., 2004b. Platinum group
1247 element geochemistry of komatiites from the Alexo and Pyke Hill areas, Ontario, Canada.
1248 Geochimica et Cosmochimica Acta 68, 1361-1383.
1249 Puchtel, I.S., Humayun, M., 2005. Highly siderophile element geochemistry of ^{187}Os-enriched
1250 2.8 Ga Kostomuksha komatiites, Baltic Shield. Geochim. Cosmochim. Acta 69, 1607-1618.
1251 Puchtel, I.S., Humayun, M., Walker, R.J., 2007. Os-Pb-Nd isotope and highly siderophile and
1252 lithophile trace element systematics of komatiitic rocks from the Volotsk suite, SE Baltic
1253 Shield. Precamb. Res. 158, 119-137.
1254 Puchtel, I.S., Walker, R.J., James, O.B., Kring, D.A., 2008. Osmium isotope and highly
1255 siderophile element systematics of lunar impact melt rocks: implications for the late
1256 accretion history of the Moon and Earth. Geochim. Cosmochim. Acta 72, 3022-3042.
1257 Puchtel, I.S., Walker, R.J., Anhaeusser, C.R., Gruau, G., 2009a. Re-Os isotope systematics and
1258 HSE abundances of the 3.5 Ga Schapenburg komatiites, South Africa: Hydrous melting or
1259 prolonged survival of primordial heterogeneities in the mantle? Chem. Geol. 262, 355-369.
1260 Puchtel, I.S., Walker, R.J., Brandon, A.D., Nisbet, E.G., 2009b. Pt-Re-Os and Sm-Nd isotope
1261 and HSE and REE systematics of the 2.7 Ga Belingwe and Abitibi komatiites. Geochim.
1262 Cosmochim. Acta 73, 6367-6389.
1263 Puchtel, I.S., Walker, R.J., Touboul, M., Nisbet, E.G., Byerly, G.R., 2014. Insights into early
1264 Earth from the Pt-Re-Os isotope and highly siderophile element abundance systematics of
1265 Barberton komatiites. Geochim. Cosmochim. Acta 125, 394-413.

1266 Raymond, S.N., Quinn, T., Lunine, J.I., 2006. High-resolution simulations of the final assembly
1267 of Earth-like planets I. Terrestrial accretion and dynamics. Icarus 183, 265–282.
1268 Raymond, S.N., Schlichting, H.E., Hersant, F., Selsis, F. 2013. Dynamical and collisional
1269 constraints on a stochastic late veneer on the terrestrial planets. Icarus 266, 671-681.
1270 Regelous, M., Elliott, T., Coath, C.D., 2008. Nickel isotope heterogeneity in the early Solar
1271 System. Earth Planet. Sci. Lett. 272, 330–338.
1272 Rehkämper, M., Halliday, A.N., Fitton, J.G., Lee, D.-C., Wieneke, M., Arndt, N.T., 1999. Ir, Ru,
1273 Pt, and Pd in basalts and komatiites: New constraints for the geochemical behavior of the
1274 platinum-group elements in the mantle. Geochim. Cosmochim. Acta 63, 3915–3934,
1275 Reufer, A., Meier, M.M.M., Benz, W., Wieler, R., 2012. A hit-and-run giant impact scenario.
1276 Icarus 221, 296-299.
1277 Righter, K., Drake, M.J., 1997. Metal-silicate equilibrium in a homogeneously accreting Earth:
1278 new results for Re. Earth Planet. Sci. Lett. 146, 541-553.
1279 Righter, K, Drake, M.J., Yaxley, G., 1997. Prediction of siderophile element metal-silicate
1280 partition coefficients to 20 GPa and 2800 degrees C: The effects of pressure, temperature,
1281 oxygen fugacity, and silicate and metallic melt compositions. Physics Earth Planet. Int.
1282 100, 115-134.
1283 Ringwood, A.E., 1966. Chemical evolution of the terrestrial planets. Geochim. Cosmochim. Acta
1284 30, 41-104.
1285 Rubie, D.C. et al., 2011. Heterogeneous accretion, composition and core–mantle differentiation
1286 of the Earth. Earth Planet. Sci. Lett. 301, 31–42.
1287 Rubie, D.C., Jacobson, S.A., Morbidelli, A., O'Brien, D.P., Young, E.D., de Vries, J., Nimmo,
1288 F., Palme, H., Frost, D.J., 2015a. Accretion and differentiation of the terrestrial planets with

implications for the compositions of early-formed Solar System bodies and accretion of water. Icarus 248, 89-108.

Rubie, D.C., Nimmo, F., Melosh, H.J. 2015b. Formation of the earth's core. In: Gerald Schubert (editor-in-chief) *Treatise on Geophysics*, 2nd edition, Oxford: Elsevier, pp. 43-79.

Ryder, G., Norman, M.D., Score, R.A., 1980. The distinction of pristine from meteorite contaminated highland rocks using metal compositions. Proc. Lunar. Planet. Sci. Conf. 11th, 471–479.

Schlichting H.E., Warren, P.E., Yin, Q.-Z., 2012. The last stages of terrestrial planet formation: dynamical friction and the late veneer. Astrophys. Journ. 752, 1-8.

Schönbächler, M., Rehkamper, M., Fehr, M.A., Halliday, A.N., Hattendorf, B., 2005. Nucleosynthetic zirconium isotope anomalies in acid leachates of carbonaceous chondrites. Geochim. Cosmochim. Acta 69, 5113-5122.

Schönbächler, M., Carlson, R.W., Horan, M.F., Mock, T.D., Hauri, E.H., 2010. Heterogeneous accretion and the moderately volatile element budget of Earth. Science 238, 884-887.

Sharp, M., Gerasimenko, I., Loudin, L.C., Liu, J., James, O.B., Puchtel, I.S., Walker, R.J., 2014. Characterization of the dominant impactor signature for Apollo 17 impact melt rock. Geochim. Cosmochim. Acta 131, 62-80.

Siebert, J., Corgne, A., Ryerson, F.J., 2011. Systematics of metal–silicate partitioning for many siderophile elements applied to Earth's core formation. Geochim. Cosmochim. Acta 75, 1451–1489.

Simon, J.I., De Paolo, D.J., 2010. Stable calcium isotopic composition of meteorites and rocky planets. Earth Planet. Sci. Lett. 289, 457–466.

1311 Spudis, P.D., Wilhelms, D.E., Robinson, M.S., 2011. The Sculptured Hills of the Taurus
1312 highlands: implications for the relative age of Serenitatis, basin chronologies and the
1313 cratering history of the Moon. Journ. Geophys. Res. 116, E00H03.
1314 Strom, R.G., Malhotra, R., Ito, T., Yoshida, F., Kring, D.A., 2005. The origin of planetary
1315 impactors in the inner solar system. Science 309, 1847-1850.
1316 Sylvester, P. J., Ward, B. J., Grossman, L., Hutcheon, I. D., 1990. Chemical compositions of
1317 siderophile element-rich opaque assemblages in an Allende inclusion. Geochim.
1318 Cosmochim. Acta 54, 3491–3508.
1319 Tagle, R., Berlin, J., 2008. A database of chondrite analysis including platinum group elements,
1320 Ni, Co, Au, and Cr: implications for the identification of chondritic projectiles. Meteor.
1321 Planet. Sci. 43, 1–19.
1322 Taylor, G.J., et al., 2006. Bulk composition and early differentiation of Mars. Journ. Geophys.
1323 Res. Planets. 111, Issue E3, Art. E03S10.
1324 Terra, F., Papanastassiou, D.A., Wasserburg, G.J., 1974. Isotopic evidence for a terminal lunar
1325 cataclysm. Earth Planet. Sci. Lett. 22, 1-21.
1326 Thiemens, M.H., Heidenreich, J.E. III., 1983. The mass-independent fractionation of oxygen: a
1327 novel isotope effect and its possible cosmochemical implications. Science 219, 1073–75
1328 Touboul, M., Puchtel, I.S., Walker, R.J., 2012. ^{182}W evidence for long-term preservation of early
1329 mantle differentiation products. Science 335, 1065–1069.
1330 Touboul, M., Liu, J., O'Neil, J., Puchtel, I.S., Walker, R.J., 2014. New insights into the Hadean
1331 mantle revealed by ^{182}W and highly siderophile element abundances of supracrustal rocks
1332 from the Nuvvuagittuq Greenstone Belt, Quebec, Canada. Chem. Geol. 383, 63–75.

1333 Touboul, M., Puchtel, I.S., Walker, R.J., 2015. Tungsten isotopic evidence for disproportional
1334 late accretion to the Earth and Moon. Nature 520, 530–533.
1335 Trinquier, A., Birck, J.-L., Allègre, C.J., 2007. Widespread ^{54}Cr heterogeneity in the inner solar
1336 system. Astrophys. Journ. 655, 1179–1185.
1337 Trinquier, A., Elliott, T., Ulfbeck, D., Coath, C., Krot, A.N., Bizzarro, M., 2009. Widespread
1338 ^{54}Cr heterogeneity in the inner solar system. Astrophys. Journ. 655, 1179–1185.
1339 Turekian K.K., Clark, S.P., 1969. Inhomogeneous accumulation of the Earth from the primitive
1340 solar nebula. Earth Planet. Sci. Lett. 6, 346-348.
1341 Turner, G., Cadogan, P.H., Yonge, C.J., 1973. Argon selenochronology. Proc. Fourth Lunar Sci.
1342 Conf., Supplement 4, Geochim. Cosmochim. Acta 2, 1889-1914.
1343 Wade, J., Wood, B.J., 2005. Core formation and the oxidation state of the Earth. Earth Planet.
1344 Sci. Lett. 236, 78– 95.
1345 Wade, J., Wood, B.J., Tuff, J., 2012. Metal–silicate partitioning of Mo and W at high pressures
1346 and temperatures: Evidence for late accretion of sulphur to the Earth. Geochim.
1347 Cosmochim. Acta 85, 58-74.
1348 Walker, R.J., Morgan, J.W., Smoliar, M.I., Beary, E., Czamanske, G.K., Horan, M.F., 1997.
1349 Application of the ^{190}Pt-^{186}Os isotope system to geochemistry and cosmochemistry.
1350 Geochim. Cosmochim. Acta 61, 4799-4808.
1351 Walker, R.J., Horan, M.F., Morgan, J.W., Becker, H., Grossman, J.N., Rubin, A., 2002a.
1352 Comparative ^{187}Re-^{187}Os systematics of chondrites: implications regarding early solar
1353 system processes. Geochim. Cosmochim. Acta 66, 4187-4201.

1354 Walker, R.J., Prichard, H.M., Ishiwatari, A., Pimentel, M., 2002b. The osmium isotopic
1355 composition of convecting upper mantle deduced from ophiolite chromitites. Geochim.
1356 Cosmochim. Acta 66, 329-345.
1357 Walker, R. J., Horan, M.F., Shearer, C.K., Papike, J.J., 2004. Depletion of highly siderophile
1358 elements in the lunar mantle: evidence for prolonged late accretion. Earth Planet. Sci. Lett.
1359 224, 399-413.
1360 Walker, R.J., 2009. Highly siderophile elements in the Earth, Moon and Mars: update and
1361 implications for planetary accretion and differentiation. Chemie der Erde 69, 101-125.
1362 Wänke, H., Dreibus G., 1988. Chemical composition and accretion history of terrestrial planets.
1363 Phil. Trans. Roy. Soc. London, Series A, 325, 545-557.
1364 Wänke, H., Dreibus G., Wright, I.P., 1994. Chemistry and accretion history of Mars. Phil. Trans.
1365 Roy. Soc. London, Series A, 349, 285-293.
1366 Wänke, H., 2001. Geochemical evidence for a close genetic relationship of Earth and Moon.
1367 Earth Moon Planets 85-6, 445-452.
1368 Warren, P.H., Wasson, J.T., 1977. Pristine nonmare rocks and the nature of the lunar crust. Proc.
1369 Lunar Sci. Conf. 8th, 2215–2235.
1370 Warren, P.H., Jerde, E.A., Kallemeyn, G.W., 1991. Pristine Moon rocks: Apollo 17 anorthosites.
1371 Proc. Lunar Planet. Sci. Conf. 21st, 51–61.
1372 Wasson, J.W., Kallemyn, G.W., 2002. The IAB iron-meteorite complex: a group, five
1373 subgroups, numerous grouplets, closely related, mainly formed by crystal segregation in
1374 rapidly cooling melts. Geochim. Cosmochim. Acta 66, 2445–2473.
1375 Wiechert, U., Halliday, A.N., Lee, D.-C., Snyder, G.A., Taylor, L.A., Rumble, D., 2001. Oxygen
1376 isotopes and the Moon-forming giant impact. Science 294, 345-348.

1377 Weidenschilling, S.J., Spaute, D., Davis, D.R., Marzari, F., Ohtsuki, K., 1997. Accretional
1378 evolution of a planetesimal swarm, Icarus 128, 429– 455.
1379 Willbold, M., Elliott, T., Moorbath, S., 2011. The tungsten isotopic composition of the Earth's
1380 mantle before the terminal bombardment. Nature 477, 195–198.
1381 Yin, Q., Jacobsen, S.B., Yamashita, K., 2002. Diverse supernova sources of pre-solar material
1382 inferred from molybdenum isotopes in meteorites. Nature 415, 881-883.
1383 Yang, J., Goldstein, J. I., Scott, E.R.D., 2008. Metallographic cooling rates of the IVA iron
1384 meteorites. Geochim. Cosmochim. Acta 70, 3197-3215.
1385 Yokoyama, T., Alexander, C.M.O'D., Walker, R.J., 2010. Osmium isotope anomalies in
1386 chondrites: results for acid residues enriched in insoluble organic matter. Earth Planet. Sci.
1387 Lett. 291, 48-59.
1388 Yurimoto, H., Kuramoto, K., 2004. Molecular cloud origin for the oxygen isotope heterogeneity
1389 in the solar system. Science 305, 1763–1766.
1390 Zhang, J., Dauphas, N., Davis, A., Leya, I., Fedkin, A., 2012. The proto-Earth as a significant
1391 source of lunar material. Nat. Geosci. 5, 251–255.
1392 Zindler, A., Hart, S., 1986. Chemical geodynamics. Ann. Rev. Earth Planet. Sci. 14, 493-571.
1393 Zinner, E., 1998. Stellar nucleosynthesis and the isotopic composition of presolar grains from
1394 primitive meteorites. Annu. Rev. Earth Planet. Sci. 26, 147–88.
1395

Figure Captions

Figure 1. CI chondrite normalized abundances of moderately and highly siderophile elements estimated for the bulk silicate Earth. Each group of siderophile elements is arranged with volatility (50% condensation temperature) increasing to the right. Estimates, together with uncertainties are taken from McDonough and Sun (1995) for the moderately siderophile elements, and from Becker et al. (2006) and Fischer-Gödde et al. (2011) for the highly siderophile elements.

Figure 2a-b. a. Molybdenum isotopic variations in iron meteorites relative to terrestrial standards, and **b.** in chondrites and shergottites. The gray fields represent the 2σ analytical uncertainties for measurements of each isotope in terrestrial standards. Error bars associated with symbols reflect the $2\sigma_M$ of data for each group. The figure is modified from Burkhardt et al. (2011).

Figure 3a-b. ^{100}Ru isotopic variations relative to terrestrial standards for **a.** iron meteorites and **b.** chondrites. The gray fields represent the 2σ analytical uncertainty for the measurements. Error bars associated with symbols reflect the $2\sigma_M$ of data for each group. The figure is modified from Chen et al. (2010).

Figure 4a-b. a. Model $\mu^{182}W$ (parts per million deviation in the $^{182}W/^{184}W$ of a sample relative to a modern terrestrial standard) evolution of the terrestrial mantle and core as a function of oligarchic growth. In the model the Moon-forming giant impact is assumed to occur 70 million years after solar system formation. It is also assumed that only 5% of the metallic core of the giant Moon-forming impactor equilibrated with the terrestrial mantle as the metal transited the silicate Earth (modified from Halliday, 2004). The increase in $\mu^{182}W$ results from the addition of the radiogenic silicate portion of the impactor to the terrestrial mantle. **b.** The same model is used as for **a**, but for this scenario 100% of the core of the giant impactor equilibrates with the silicate Earth (modified from Halliday, 2008). The decrease in $\mu^{182}W$ results from the addition of metal with appreciable W and very low $\mu^{182}W$ (-200) from the core of the impactor to the terrestrial mantle.

Figure 5. Variance in HSE ratios and $^{187}Os/^{188}Os$, which serves as a proxy for long-term Re/Os, in the major primitive meteorite groups. Data for bulk chondrites are from Walker et al. (2002a), Horan et al. (2003), Brandon et al. (2005) and Fischer-Gödde et al. (2010). Also shown is the estimate for the BSE from Becker et al. (2006).

Figure 6a-d. Histogram plot of $^{187}Os/^{188}Os$ data for bulk chondrites compared with the minimum estimate for the BSE. Chondrite data are from Walker et al. (2002a), Brandon et al. (2005) and Fischer-Gödde et al. (2010). BSE ratio is taken from Meisel et al. (2001).

Figure 7. Plot of the concentrations of HSE estimated for the BSE doubly normalized to CI chondrite concentrations and the Ir/CI in BSE. The normalizing CI data are for Orgueil reported in Horan et al. (2003) and Fischer-Gödde et al. (2010). The ranges of normalized concentrations for the three major chondrite groups are also from Horan et al. (2003) and Fischer-Gödde et al. (2010). Data for BSE are from Becker et al. (2006) and Fischer-Gödde et al. (2011).

Figure 8. Calculated total Pt+Pd abundances in the sources of Archean komatiites as compared to the BSE estimate of Becker et al. (2006). For each of these systems, ^{187}Re-^{187}Os isochrons consistent with the known ages of the rocks have been generated, consistent with closed-system behavior for other HSE. The late Archean komatiite systems span a substantial range, from 58±7% in the 2.69 Ga Belingwe system to 85±5% in the 2.72 Ga Abitibi system, of the total Pt and Pd present in the estimates for the modern BSE, with the 2.41 Ga Vetreny system being at the lower end of this range. Within the uncertainties, the total Pt+Pd abundances in some of the late Archean komatiite systems, e.g., Abitibi and Kostomuksha, overlap with those in the estimates for the BSE, whereas in the others (Vetreny, Belingwe, and Volotsk-Kamennoozero) fall slightly (by 20-14% when the full uncertainties on the estimates are considered) short of reaching that level. The total Pt+Pd abundances in the sources of the two out of three early Archean komatiite systems from the Barberton Greenstone Belts, South Africa, are within the range of those in the late Archean komatiite systems, albeit on the lower side, varying from 56±12% for the Komati to 65±10% for the Weltevreden, of the total Pt+Pd present in the estimates for the modern BSE, whereas the third system (Schapenburg) is characterized by much lower Pt+Pd abundances (27±4% of BSE). Data sources: Puchtel et al. (2004a,b; 2005; 2007; 2009a,b; 2014), and Puchtel and Humayun (2005).

Figure 9a-b. a. Platinum concentration versus MgO data for lunar volcanic rocks (colored symbols), compared to data for terrestrial basalts, picrites, komatiites and peridotites (gray symbols). Lunar data are from Walker et al. (2004) and Day et al. (2007). **b.** Platinum concentration versus MgO data for martian shergottites (red symbols) compared to terrestrial basalts, picrites, komatiites and peridotites (gray symbols). Shergottite data are from Brandon et al. (2012).

Figure 10. Plot of $\mu^{182}W$ values for ancient rocks from the ≥3.8 Ga Nuvvuagittuq, Quebec, supracrustal suite, the ~3.7 Ga supracrustal rocks from Isua, Greenland, the 3.5 Ga Komati komatiites from the Barberton Greenstone Belt, South Africa, and 2.8 Ga komatiites from Kostomuksha, Fennoscandia. Data are from Willbold et al. (2011), Touboul et al. (2012) and Touboul et al. (2014).

Figure 11. Plot of ^{92}Mo versus ^{100}Ru of group averages chondrites and iron meteorites showing the linear trend defining *s*-process enriched and depleted compositions. Note that Earth plots at one end of the trend. Data are from Burkhardt et al. (2011) and Chen et al. (2010).

Figure 12. Plot of Re, Os, Ru, Pt, and Pd versus Ir for six pieces of Apollo 14 impact melt rock 14321. The linear trends and zero intercepts are consistent with two component mixing of HSE in these rock fragments. One component is presumed to be pristine lunar crust with very low HSE abundances, and the second component appears to be a chondritic impactor with high HSE

abundances. The slopes of the trends likely define the HSE/Ir ratios of the basin forming impactor associated with this site. Figure is modified from Puchtel et al. (2008).

Figure 13a-d. Plots of **a.** Ru/Ir, **b.** Pt/Ir, **c.** Pd/Ir, and **d.** Os/Ir ratios versus $^{187}Os/^{188}Os$ (proxy for long term Re/Os) for impact melt rocks from Apollo 14, 15, 16 and 17 landing sites, as well as two lunar meteorites. Each datum represents the regression of data for multiple fragments of each rock (e.g., Figure 12 for sample 14321). The error bars on the vertical axes represent the 2σ regression uncertainties for each rock. The error bars on the horizontal axes reflect the range of $^{187}Os/^{188}Os$ among subsamples of each rock. Data are from: Puchtel et al. (2008); Fischer-Gödde and Becker (2012); Sharp et al. (2014) and Liu et al. (2015). Open symbols are data for bulk chondrites as shown in Figure 5. Figure is modified from Liu et al. (2015).

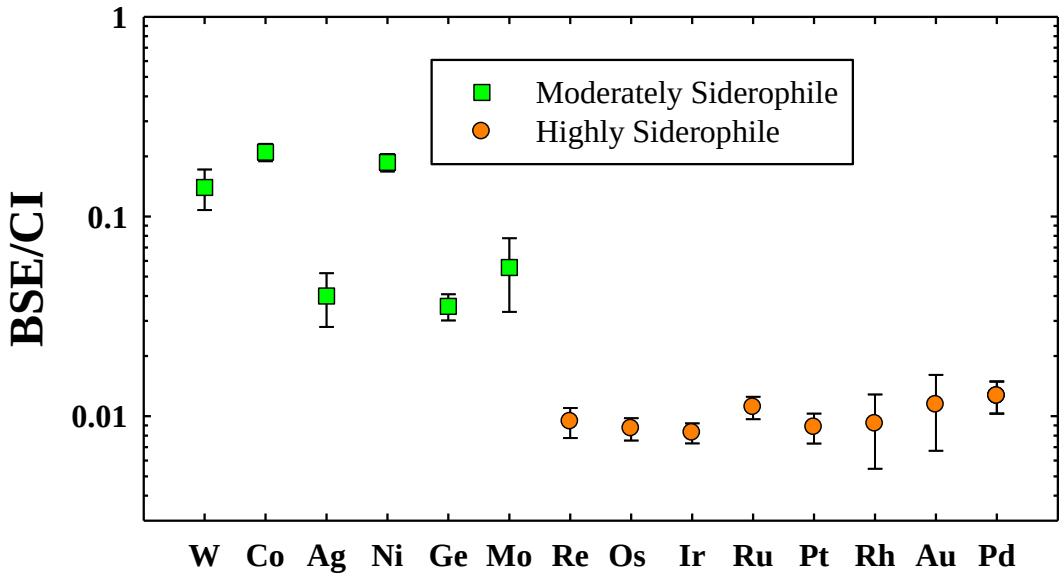
1
0.1
0.01
BSE/CI
Moderately Siderophile
Highly Siderophile
W
Co
Ag
Ni
Ge
Mo
Re
Os
Ir
Ru
Pt
Rh
Au
Pd

Figure 1.

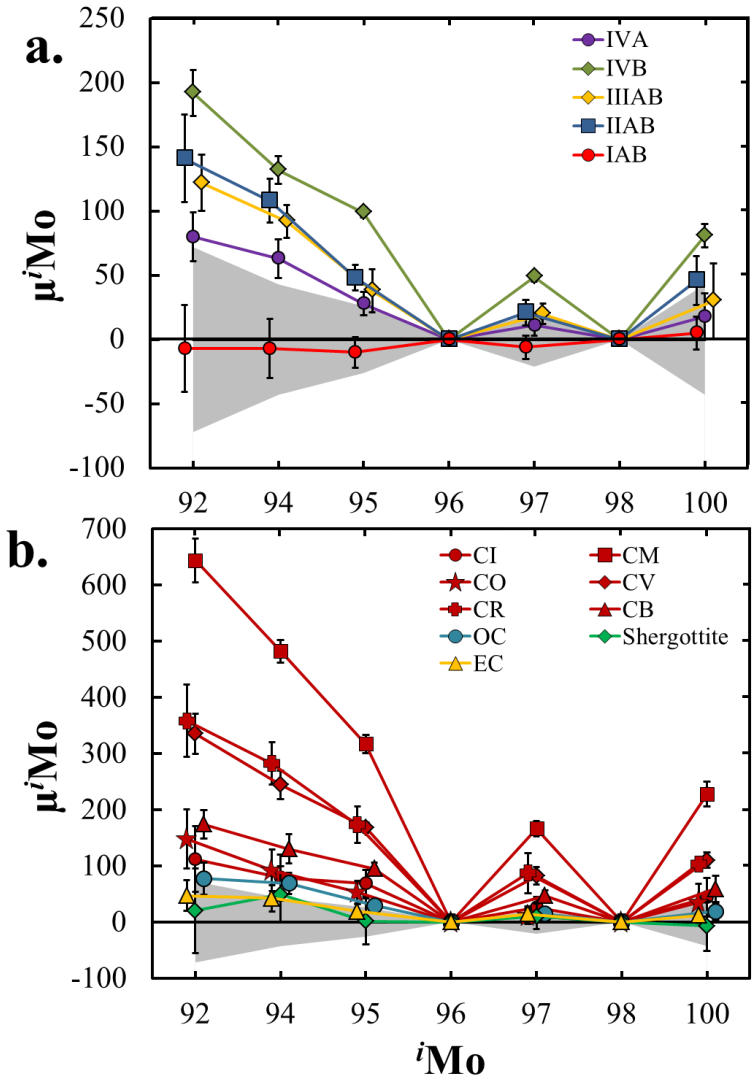
a.
IVA
IVB
IIIAB
IIAB
IAB
μiMo
250
200
150
100
50
0
-50
-100
92
94
95
96
97
98
100
b.
CI
CM
CO
CV
CR
CB
OC
Shergottite
EC
μiMo
700
600
500
400
300
200
100
0
-100
92
94
95
96
97
98
100
iMo

Figure 2a-b.

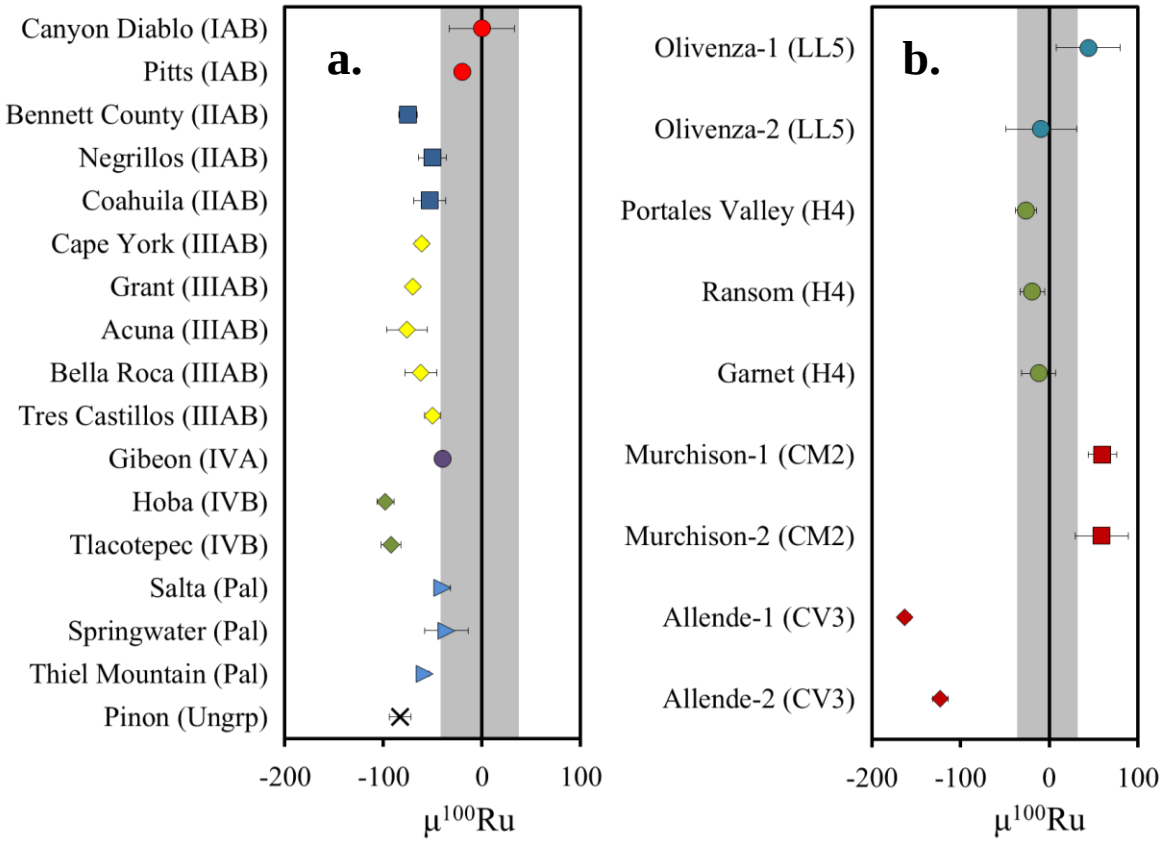
a.
Canyon Diablo (IAB)
Pitts (IAB)
Bennett County (IIAB)
Negrillos (IIAB)
Coahuila (IIAB)
Cape York (IIIAB)
Grant (IIIAB)
Acuna (IIIAB)
Bella Roca (IIIAB)
Tres Castillos (IIIAB)
Gibeon (IVA)
Hoba (IVB)
Tlacotepec (IVB)
Salta (Pal)
Springwater (Pal)
Thiel Mountain (Pal)
Pinon (Ungrp)
-200
-100
0
100
μ100Ru
b.
Olivenza-1 (LL5)
Olivenza-2 (LL5)
Portales Valley (H4)
Ransom (H4)
Garnet (H4)
Murchison-1 (CM2)
Murchison-2 (CM2)
Allende-1 (CV3)
Allende-2 (CV3)
-200
-100
0
100
μ100Ru

Figure 3a-b.

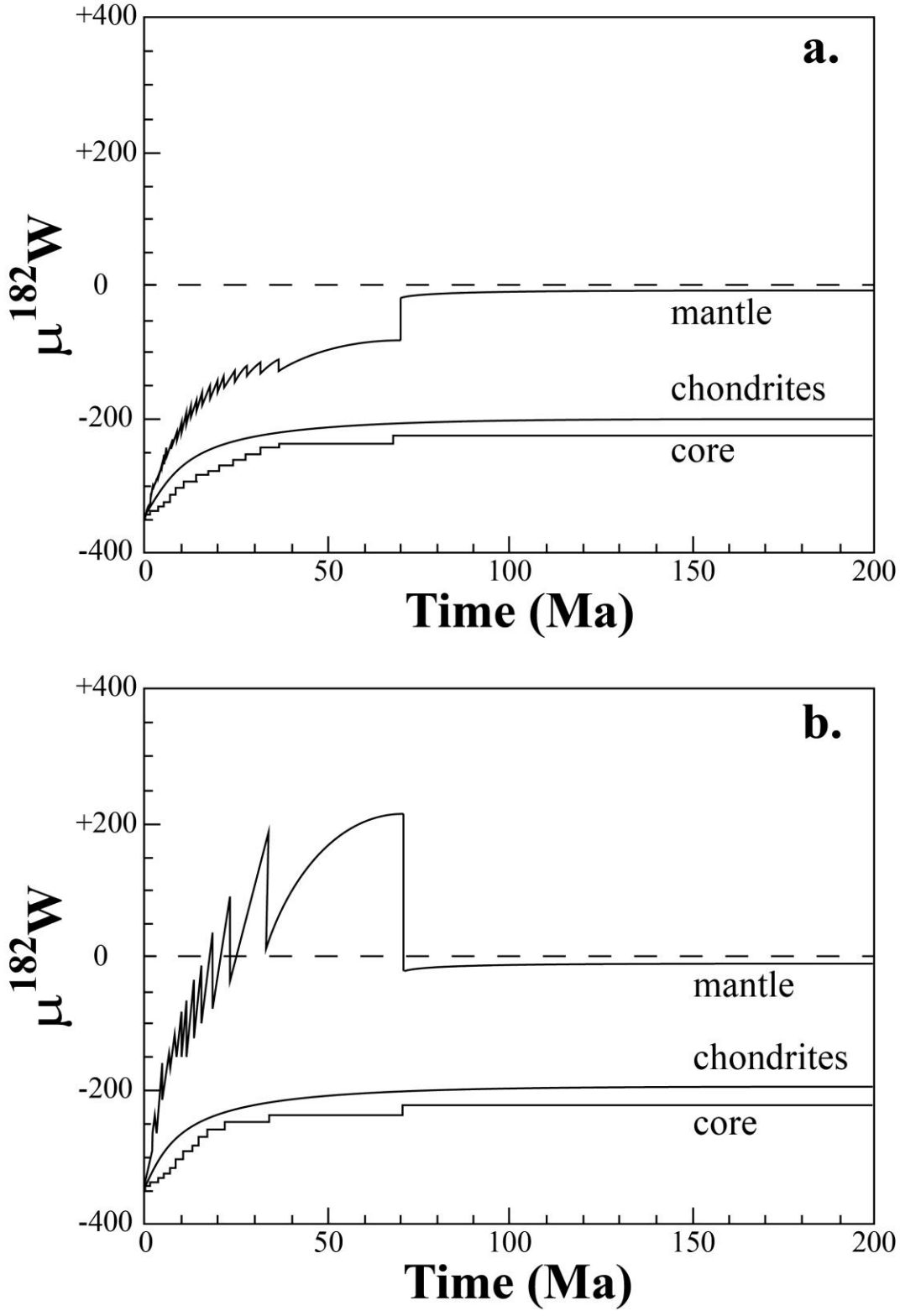
a.
+400
+200
0
-200
-400
μ182W
mantle
chondrites
core
0
50
100
150
200
Time (Ma)
b.
+400
+200
0
-200
-400
μ182W
mantle
chondrites
core
0
50
100
150
200
Time (Ma)

Figure 4a-b.

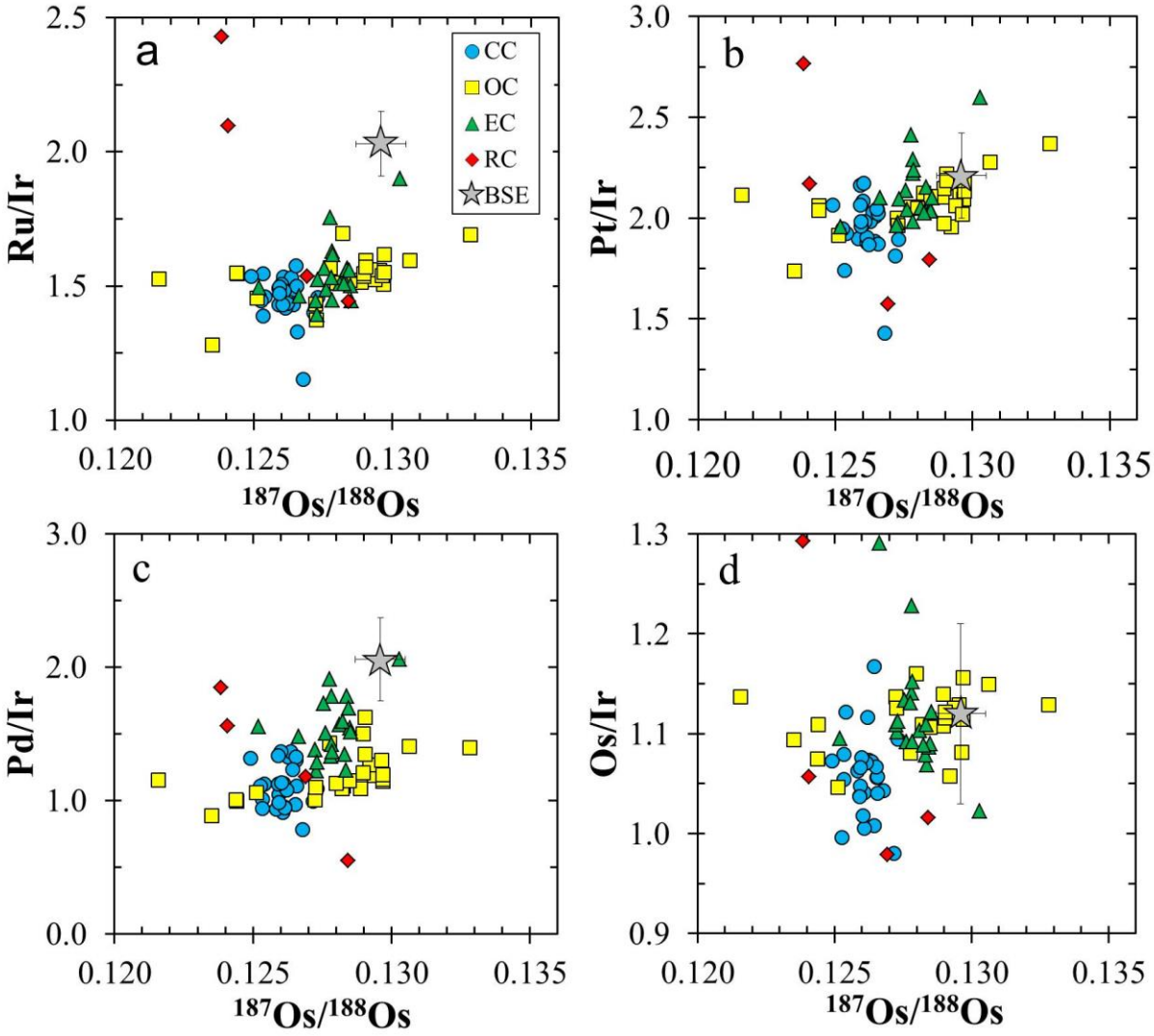
a
CC
OC
EC
RC
BSE
Ru/Ir
2.5
2.0
1.5
1.0
0.120
0.125
0.130
0.135
187Os/188Os
b
Pt/Ir
3.0
2.5
2.0
1.5
1.0
187Os/188Os
c
Pd/Ir
3.0
2.0
1.0
0.0
187Os/188Os
d
Os/Ir
1.3
1.2
1.1
1.0
0.9
187Os/188Os

Figure 5a-d.

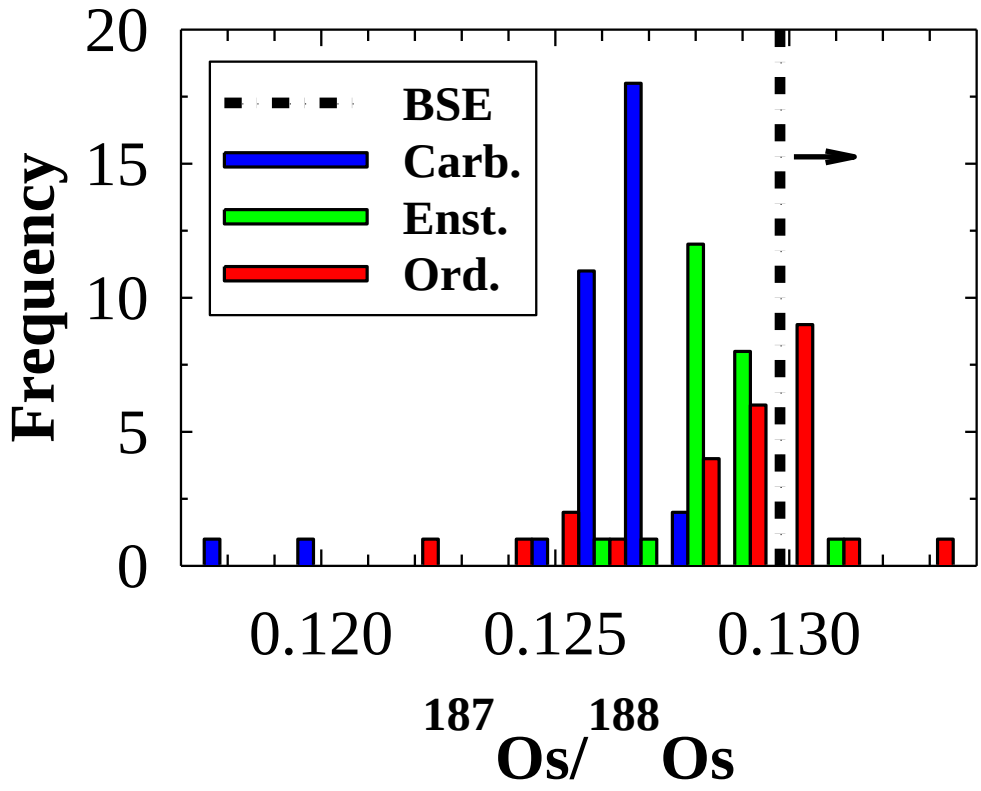
20
15
10
5
0
Frequency
BSE
Carb.
Enst.
Ord.
0.120
0.125
0.130
187
Os/
188
Os

Figure 6.

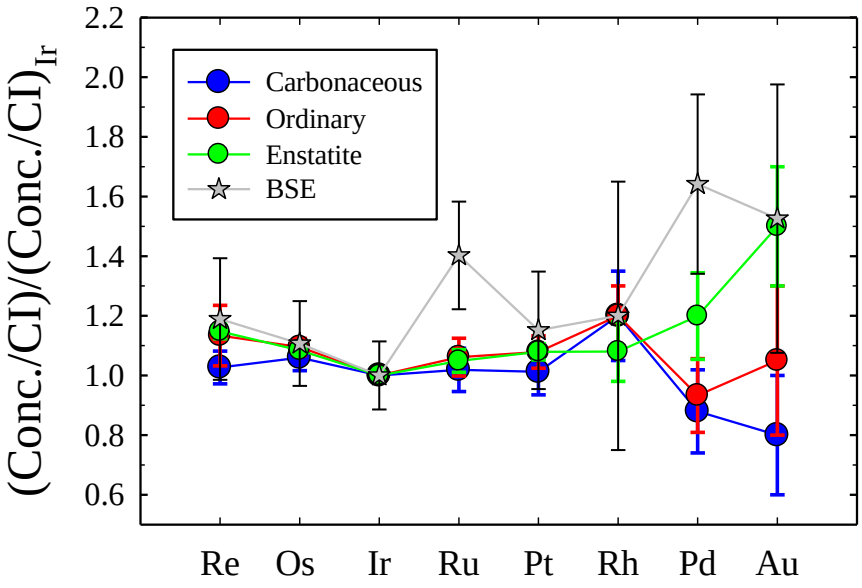

1543

1544

1545 **Figure 7.**

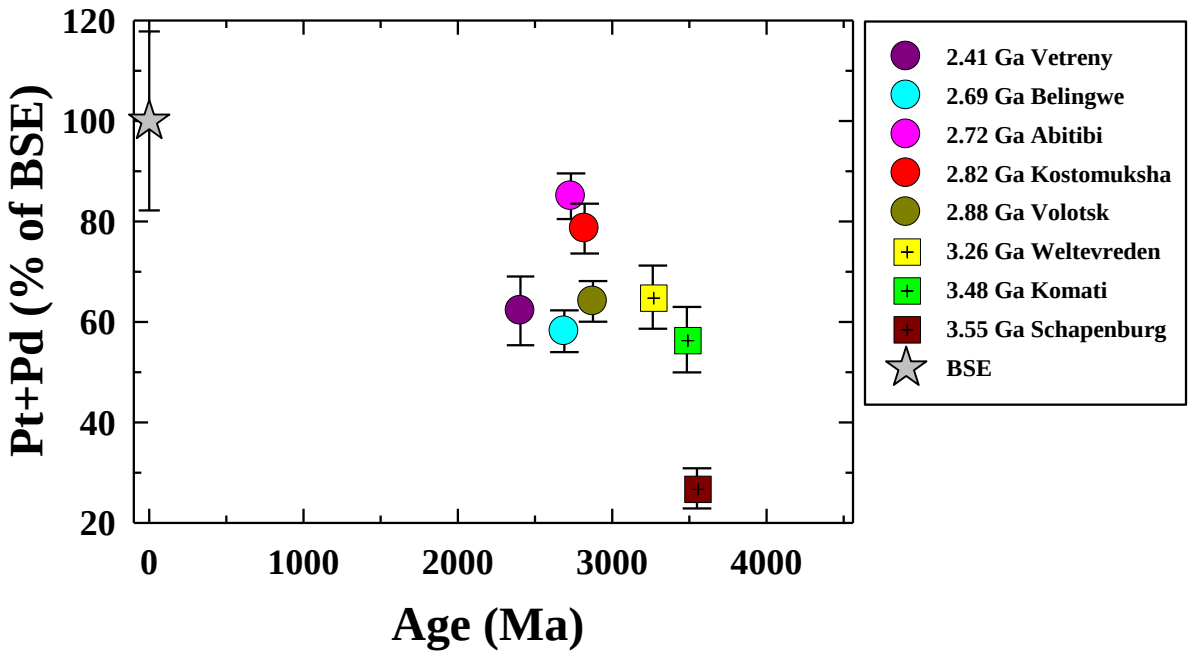
Pt+Pd (% of BSE)
120
100
80
60
40
20
0
1000
2000
3000
4000
Age (Ma)
2.41 Ga Vetreny
2.69 Ga Belingwe
2.72 Ga Abitibi
2.82 Ga Kostomuksha
2.88 Ga Volotsk
3.26 Ga Weltevreden
3.48 Ga Komati
3.55 Ga Schapenburg
BSE

Figure 8.

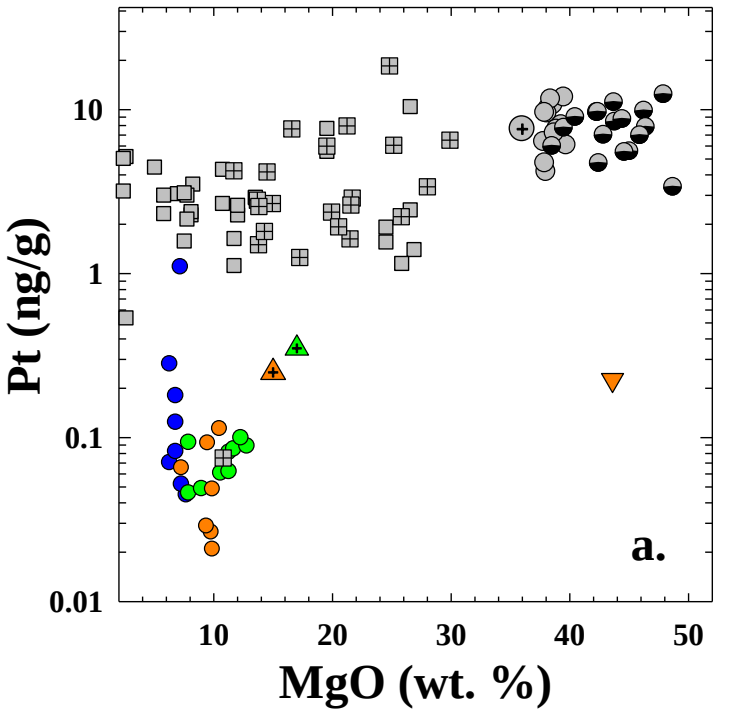
Pt (ng/g)
10
1
0.1
0.01
10
20
30
40
50
MgO (wt. %)
a.

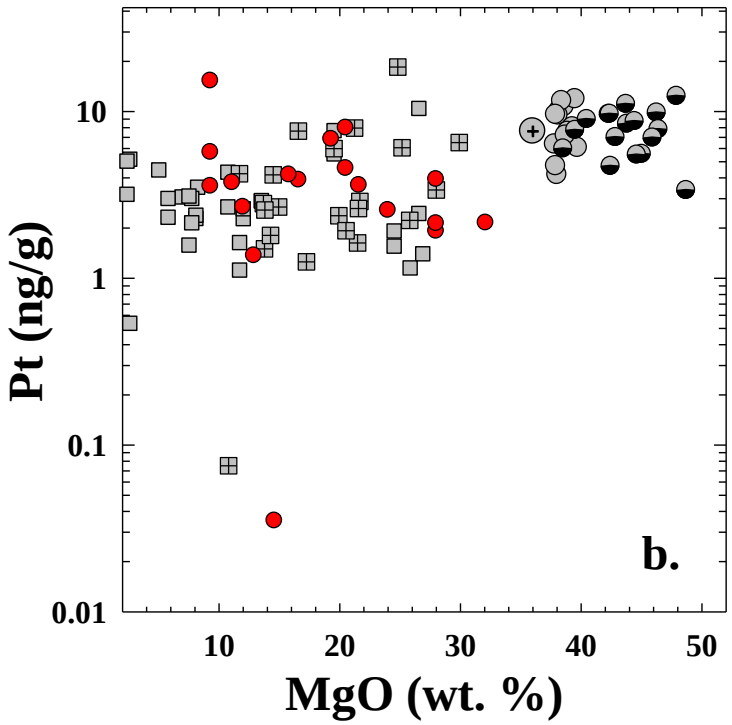
Pt (ng/g)
10
1
0.1
0.01
10
20
30
40
50
MgO (wt. %)
b.

Figure 9a-b.

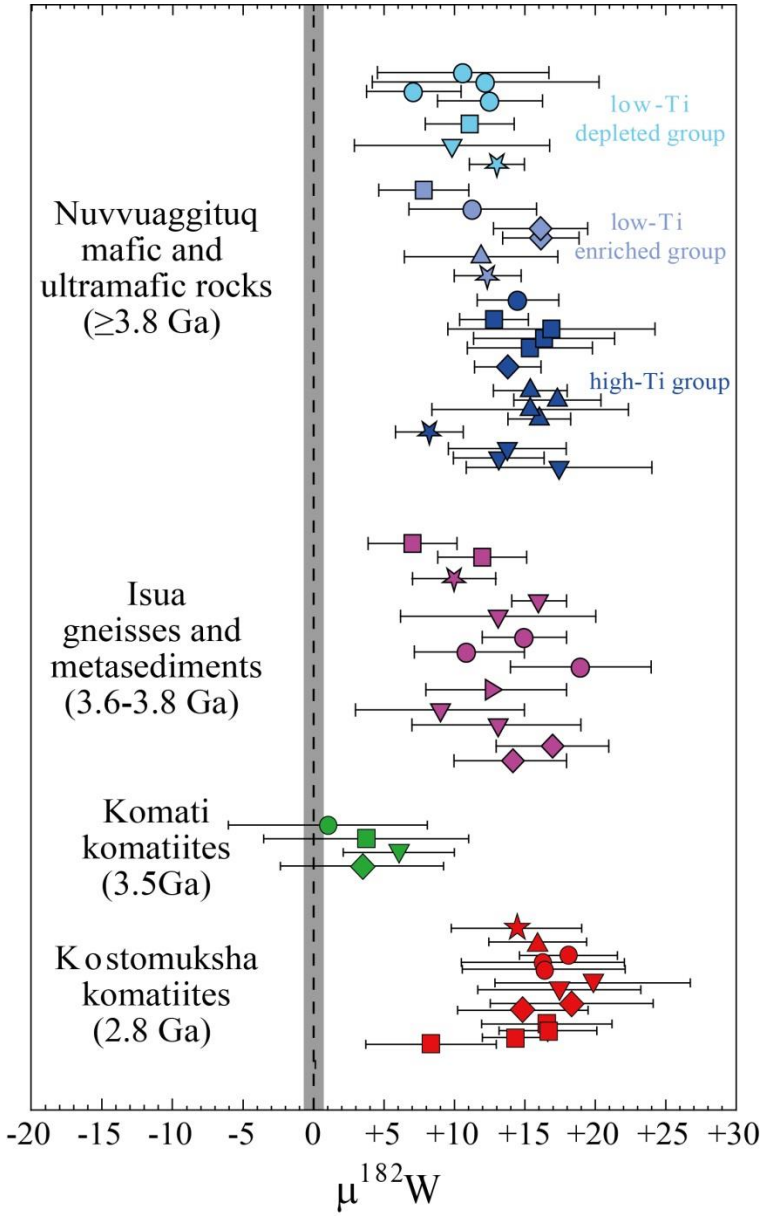
Nuvvuaggituq
mafic and
ultramafic rocks
(≥3.8 Ga)
low-Ti
depleted group
low-Ti
enriched group
high-Ti group
Isua
gneisses and
metasediments
(3.6-3.8 Ga)
Komati
komatiites
(3.5Ga)
Kostomuksha
komatiites
(2.8 Ga)
-20 -15 -10 -5 0 +5 +10 +15 +20 +25 +30
μ182W

Figure 10.

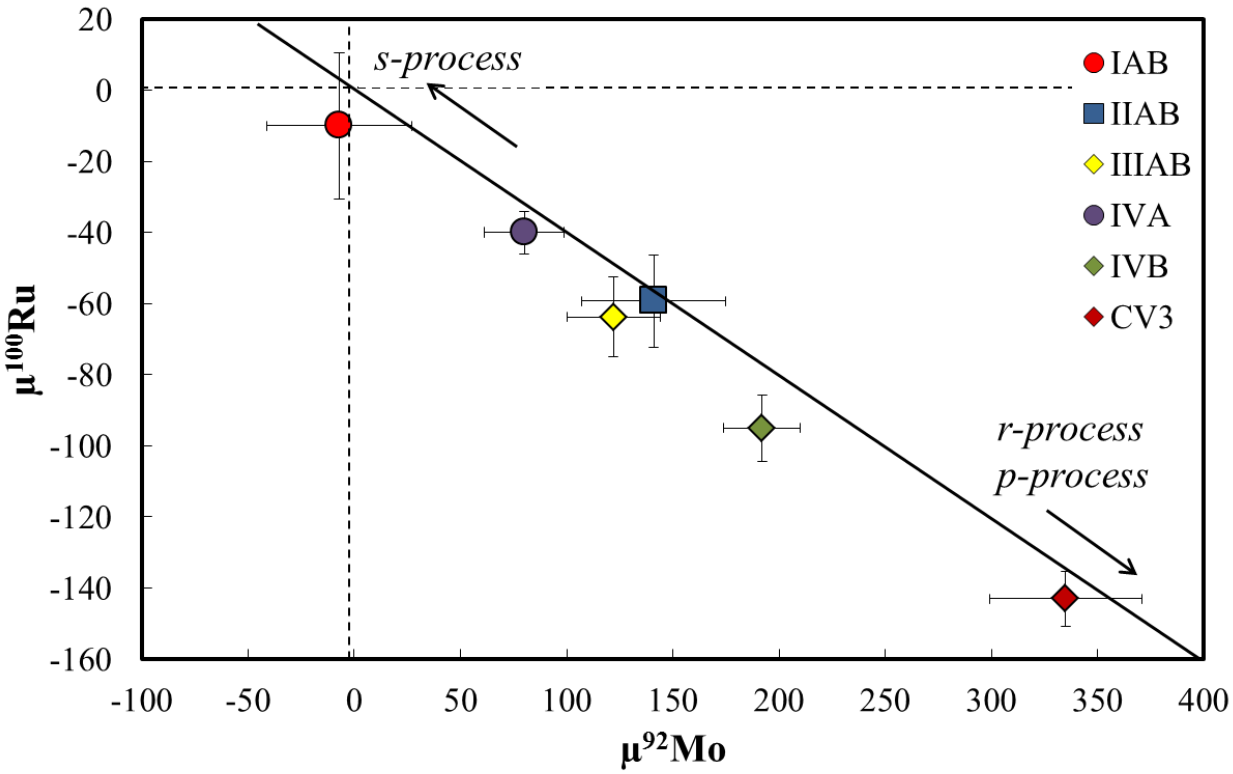
s-process
r-process
p-process
IAB
IIAB
IIIAB
IVA
IVB
CV3
μ100Ru
μ92Mo
20
0
-20
-40
-60
-80
-100
-120
-140
-160
-100
-50
0
50
100
150
200
250
300
350
400

Figure 11.

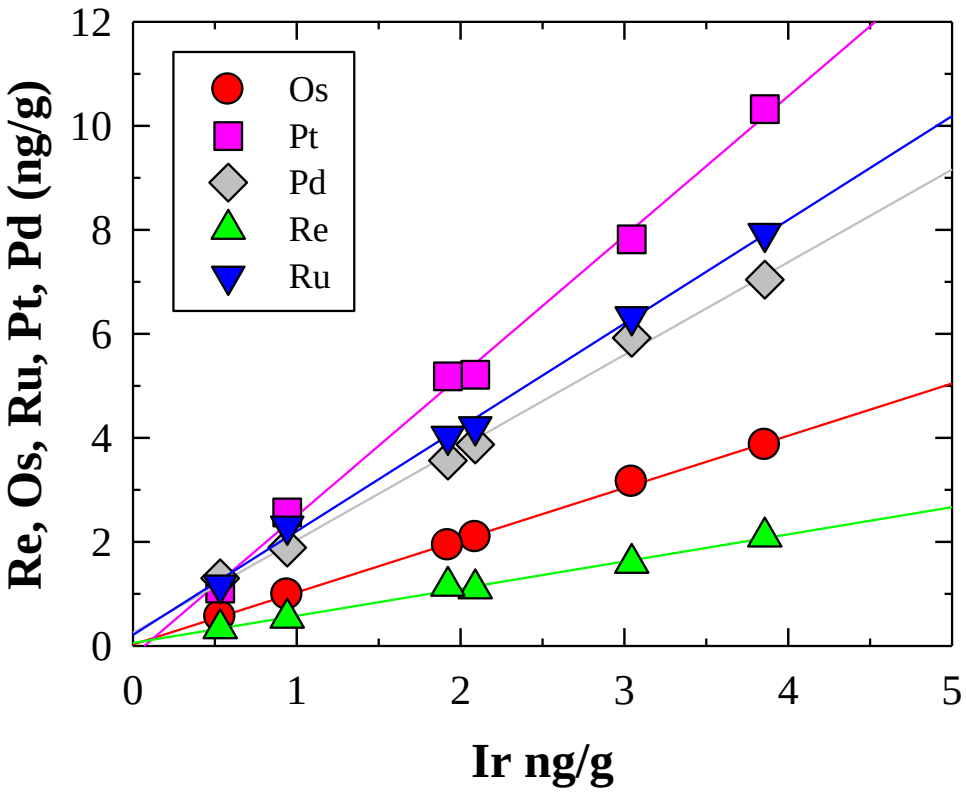

Figure 12.

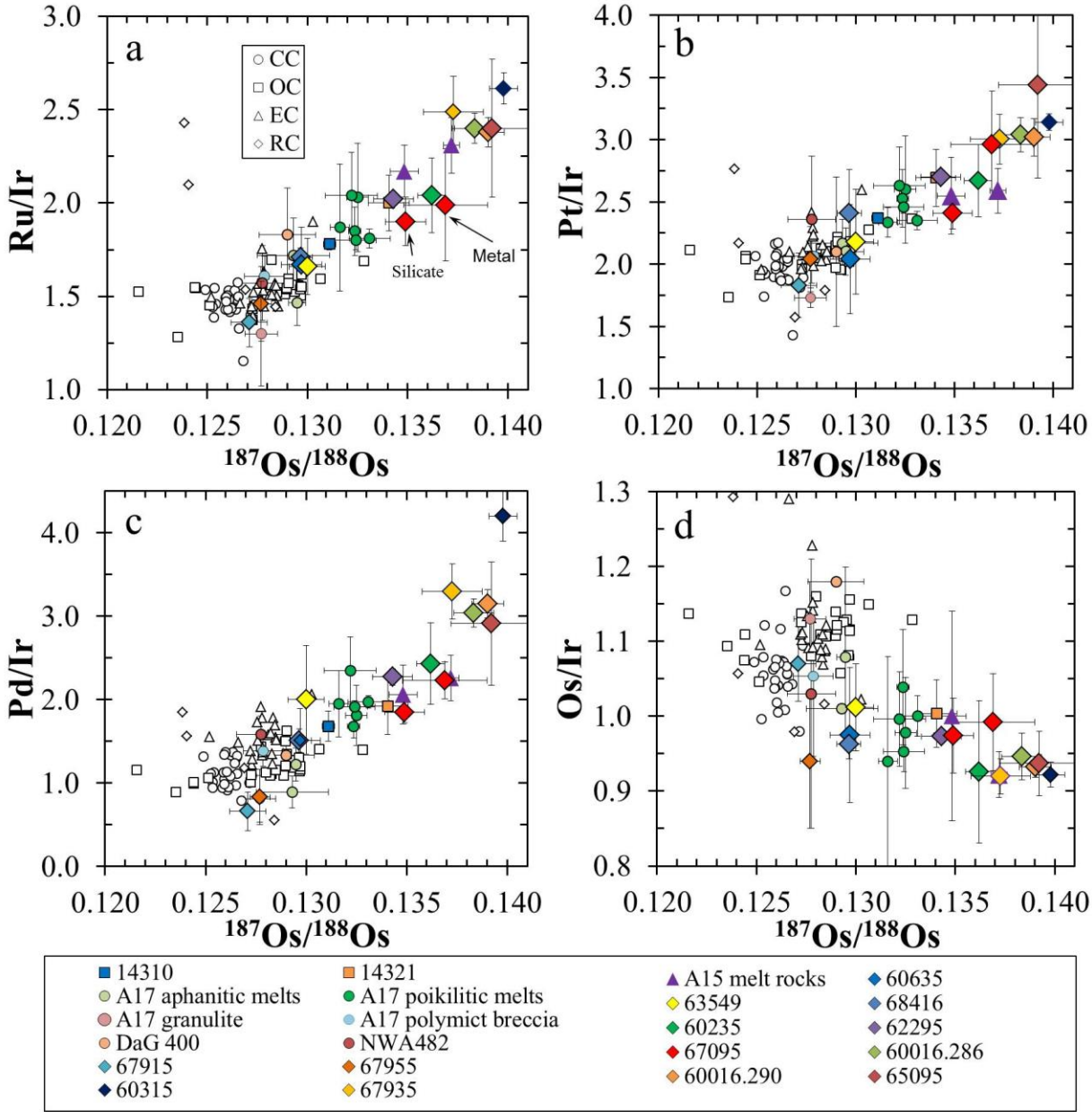
a
CC
OC
EC
RC
Silicate
Metal
Ru/Ir
187Os/188Os
b
Pt/Ir
187Os/188Os
c
Pd/Ir
187Os/188Os
d
Os/Ir
187Os/188Os
14310
14321
A15 melt rocks
60635
A17 aphanitic melts
A17 poikilitic melts
63549
68416
A17 granulite
A17 polymict breccia
60235
62295
DaG 400
NWA482
67095
60016.286
67915
67955
60016.290
65095
60315
67935

Figure 13a-d.